Journal of Medicinal Chemistry

pubs.acs.org/jmc

Article

Discovery of HN37 as a Potent and Chemically Stable Antiepileptic Drug Candidate

Yang-Ming Zhang,[⊥] Hai-Yan Xu,[⊥] Hai-Ning Hu,[⊥] Fu-Yun Tian, Fei Chen, Hua-Nan Liu, Li Zhan, Xiao-Ping Pi, Jie Liu, Zhao-Bing Gao,* and Fa-Jun Nan*

Cite This: *J. Med. Chem.* 2021, 64, 5816−5837

Read Online

ACCESS | Metrics & More | Article Recommendations | Supporting Information

ABSTRACT: We previously reported that P-retigabine (P-RTG), a retigabine (RTG) analogue bearing a propargyl group at the nitrogen atom in the linker of RTG, displayed moderate anticonvulsant efficacy. Recently, our further efforts led to the discovery of **HN37** (pynegabine), which demonstrated satisfactory chemical stability upon deleting the ortho liable $-NH_2$ group and installing two adjacent methyl groups to the carbamate motif. **HN37** exhibited enhanced activation potency toward neuronal Kv7 channels and high *in vivo* efficacy in a range of pre-clinical seizure models, including the maximal electroshock test and a 6 Hz model of pharmacoresistant limbic seizures. With its improved chemical stability, strong efficacy, and better safety margin, **HN37** has progressed to clinical trial in China for epilepsy treatment.

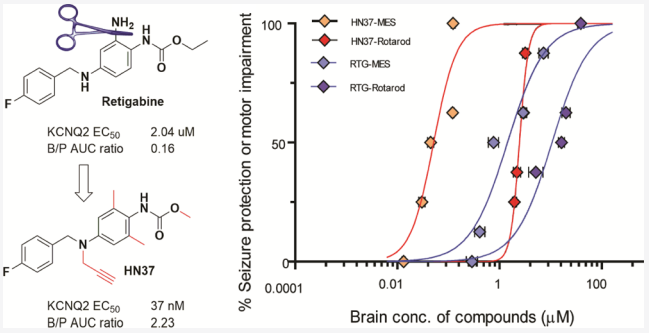

INTRODUCTION

Epilepsy is one of the most common neurological disorders that is characterized by recurrent, unprovoked seizures and affects up to 70 million people worldwide. It usually manifests as disturbances of perception, motor control, consciousness, or autonomic control and frequently results in serious morbidity and high mortality. Epilepsy is a severe threat to patients' quality of life and well-being and exerts a heavy burden on their families.[1]

Nowadays, antiepileptic drugs (AEDs) are the mainstay treatment for epilepsy with over 30 AEDs approved for clinical use. Unfortunately, about 30% of patients do not respond to these AEDs despite the practice of increasing drug dosage or using combination therapies.[2,3] While the mechanisms of epilepsy pharmacoresistance continue to be investigated, more effective AEDs, particularly with novel mechanisms of actions and reduced side effects are still in high demand as an additional medication option, especially for patients with treatment-resistant epilepsy or treatment-refractory seizures.[4−6]

Voltage-gated K^+ channels (Kv) play crucial roles in regulating intrinsic electrical properties in excitable cells. As the seventh member of Kv channels, the K_V7 family includes five members (Kv7.1-5) encoded by KCNQ1−5 genes and has gained widespread interest due to its link to diseases and overall tractability as drug targets.[7] While KCNQ1 is confined in cardiac tissues and co-assembled with KCNE1, KCNQ2−5 are mainly expressed in central and peripheral nervous systems and therefore often referred to as neuronal KCNQs. Among neuronal KCNQs, KCNQ2 and KCNQ3 subunits can assemble into KCNQ2/3 heterotetramers, which have been identified as the main molecular entities of M-currents. As M-current can function as a brake to firing in neurons, activators of neuronal KCNQ channels may have valuable applications for developing novel AEDs.[8−10] This concept was validated by the approval of retigabine (RTG) in 2011, the first neuronal Kv7 agonist, marketed as Potigar in USA and Trobalt in Europe for adjunctive treatment of partial-onset seizures.[8] In a key clinical trial, RTG was efficacious in patients who suffered from inadequate seizure control using other AEDs. The average seizure frequency was reduced by 23−28, 29−40, and 35−44% at 600, 900, and 1200 mg/day, respectively, compared with the placebo group (13−18%).[9,10] This drug was particularly efficacious for a small group of children with an aberrant KCNQ2 gene.[11]

Most clinical adverse events of RTG include dizziness, fatigue, confusion, vertigo, and tremor.[9,12] In addition, RTG may cause a unique adverse effect, urinary retention, presumably due to potentiating KCNQ channels expressed in bladder tissues.[13−15] However, in 2013, case reports of skin discolorations on peripheral tissues aroused much safety

Received: December 29, 2020
Published: April 30, 2021

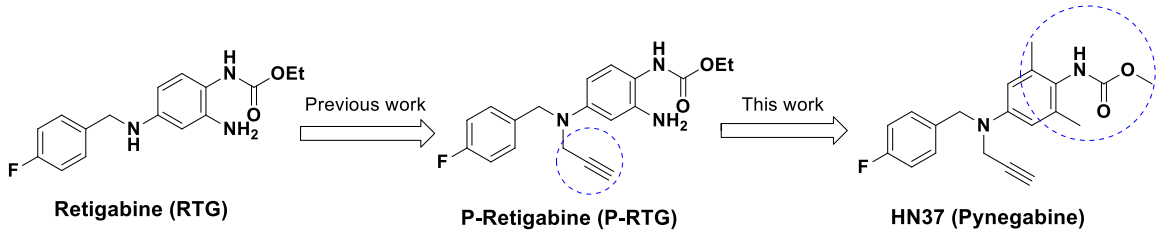

Figure 1. Structures of retigabine, P-retigabine, and HN37 (Pynegabine).

Scheme 1. Synthesis of Deaminated Analogues of P-RTG (L1-1 to L1-8) with a Variety of *N*-Acyl Groups

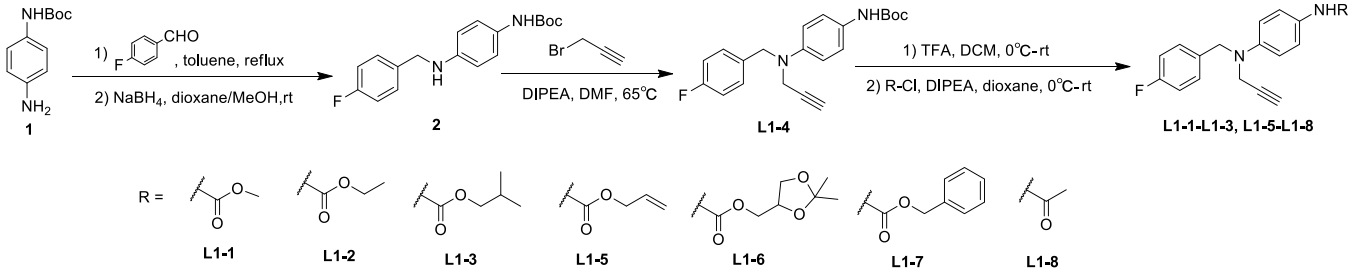

concern with its long-term use.[16−19] Though most discolorations are reversible, the potential loss of vision due to retinal discoloration eventually led to a black box warning on RTG medication. Eye examination every 6 months is recommended under RTG treatment.[18] Although the European Medicines Agency (EMA) and the US FDA acknowledge that the benefits of RTG therapy outweigh its potential risks, Potigar and Trobalt have been discontinued in all markets since June 2017 on account of decreased commercial prospects.

Research on RTG-related discolorations suggests that melanin accelerates the pigmentation process caused by dimerization of RTG and its *N*-acetyl metabolite (NAMR).[16,20−22] Through its binding to both RTG and NAMR, melanin enriches their concentrations and provides appropriate structural conformations to initiate their dimerization.[21] Pigmented dimers of RTG and NAMR were found in the eye and skin of pigmented rats as well as in biopsy samples from human subjects.[21] As the pigmentation seems unrelated to its mechanism of action, attention has been turned toward its polyaminobenzene structure. It is reported that RTG tends to dimerize through forming two possible *p*-quinone diimines, the potential reactive intermediates playing key roles in forming dimers and readily reacting with a variety of substrates *in vivo*.[23−25] Self-coupling of polyaminobenzenes has long been applied in oxidative hair dye formation. Earlier, flupirtine, a non-opiate analgesic having a similar structure, was reported to produce some dimeric metabolites.[26]

To address these undesirable side effects, novel candidates are developed by substitution on the primary $-NH_2$ group, forming piperidines to increase the steric hindrance, synthesis of sulfide analogues, enhancement of subtype selectivity toward the KCNQ family, and providing conformationally restricted RTG analogues.[20,24,27−32] In particular, several di-ortho-methyl-substituted RTG analogues have been reported as promising novel Kv7 activators. For example, Yang et al. developed a series of piperidine-based di-ortho-methyl-substituted butanamides using a hybridization drug design strategy.[33,34] Recently, Zhang et al. reported a novel potent neuronal Kv7 channel opener SCR2682 also containing two ortho methyl substituents.[35,36] Besides, compound XEN1101 (1OP-2198), one of a series of 4-(*N*-azacycloalkyl) anilides with two ortho methyl substituents, has progressed into Phase 2 clinical trial to treat focal epilepsy (ClinicalTrials.gov Identifier: NCT03796962).[37−39]

Both RTG and flupirtine share a motif of arene ortho-diamines with one acylated and another as an unsubstituted primary amine. This motif seems critical for potentiating KCNQ channels as the deaminated version of RTG (compound **K3**) shows much reduced potency.[40] This SAR (structure−activity relationship) information, on the other hand, presents an opportunity for improving chemical stability by deleting the adjacent liable $-NH_2$ group, if potency is maintained or even improved.

In our previous work, we discovered a RTG derivative, P-retigabine (P-RTG, ethyl *N*-[2-amino-4-((4-fluorobenzyl) (prop-2-ynyl)amino)phenyl]carbamate, Figure 1), which incorporated a propargyl group at the nitrogen atom in the linker of RTG.[41] P-RTG (ED_{50} = 6.5 mg/kg) displayed more potent antiepileptic efficacy in the maximal electroshock (MES) mouse model than RTG (ED_{50} = 15.0 mg/kg). In addition, P-RTG exhibited an inverted brain-to-blood drug distribution probably due to increased lipophilicity. This inverted brain-to-blood drug distribution might be beneficial for CNS drugs, if it could enhance efficacy and reduce side effects. However, the concern about its chemical instability for the triaminobenzene structure impedes its further pre-clinical development.[20,21,23,24]

Enlightened by the maintained anticonvulsant potency of P-RTG, we therefore undertook further structural explorations and modifications on the basis of retaining the propargyl group. The propargyl group enhanced the tolerance toward structural modifications probably due to its potential for $\pi-\pi$ stacking with aromatic moieties in its binding pocket, thus opening a new avenue for modifying RTG structures. Herein, we describe our recent efforts which led to the discovery of methyl (4-((4-fluorobenzyl) (prop-2-yn-1-yl) amino)-2, 6-dimethylphenyl) carbamate (**HN37**, pynegabine, Figure 1) as a promising antiepileptic drug candidate. It displays satisfactory chemical stability by deleting the liable ortho $-NH_2$ and installing two neighboring methyl groups to the carbamate functionality. In its pre-clinical study, **HN37** exhibits enhanced efficacy and a better safety margin than RTG. As a new

https://doi.org/10.1021/acs.jmedchem.0c02252
J. Med. Chem. 2021, 64, 5816−5837

Scheme 2. Synthesis of Deaminated Analogues of P-RTG (L2-1 to L2-8) with a Variety of Substituents on the Left Benzene Ring

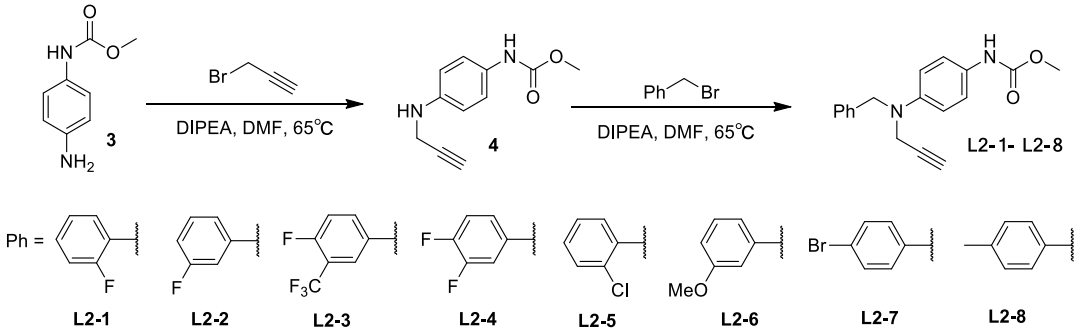

generation of Kv7 activator, **HN37** is an ideal drug candidate for treating epilepsy and pursuing other indications.

DESIGN AND CHEMISTRY

As our first approach to improve chemical stability, the liable ortho $-NH_2$ substituent in P-RTG was first removed and a series of analogues with a variety of *N*-acyl motifs were designed and synthesized (Scheme 1). Intermediate **2**, readily obtained by the reductive amination of aniline **1** with *p*-fluorobenzaldehyde, was reacted with propargyl bromide to afford the corresponding compound **L1-4**, which was further transformed into amine and reacted with various acylating agents to afford the deaminated analogues **L1-1** to **L1-3** and **L1-5** to **L1-8**.

Next, modifications of the left benzene ring of P-RTG were carried out through the synthesis of compounds **L2-1** to **L2-8** (Scheme 2). Intermediate **4**, prepared by the reaction of methyl (4-aminophenyl) carbamate **3** with propargyl bromide, was subsequently reacted with a variety of benzyl bromides to afford compounds **L2-1** to **L2-8**.

Structural scanning and optimization toward the substituents on the right benzene ring of P-RTG were achieved through the synthesis of *o*-, *m*-, and *p*-methoxycarbonylaminio-substituted analogues (**L3-1** to **L3-15**) using various diaminobenzenes or nitro-aminobenzenes (**5a**−**5k**) through regular functional group protections and transformations (Schemes 3 and 4).

RESULTS AND DISCUSSION

Structure−Activity Relationship Study. The chemical instability of RTG mainly arises from its electron-rich polyaminobenzene structure which is further exacerbated by an ortho $-NH_2$ substituent. A similar motif of this ortho-diamine arene with one acylated amine and one primary amine is also observed in some CNS drugs, such as flupirtine, a nonopiate analgesic with decades of clinical use in Germany. This motif seems to be a critical pharmacophore for potentiating KCNQ channels as the deaminated version of RTG (compound **K3**) displays much reduced potency compared with RTG.[40] The identifications of some pigmented RTG-related dimers in melanin-rich tissues suggest an association with the polyaminobenzene structure of RTG which tends to form active intermediates and produces pigmented dimers in an oxidative environment. Actually, some dark-blue precipitates could be observed several hours later when aqueous solution of RTG dihydrochloride was stirred in an open flask at ambient temperatures (unpublished data). Enlightened by our previous work of incorporating a propargyl group into RTG, we initiated further structure scanning and modifications on the basis of retaining the propargyl group in order to address RTG-associated issues of discoloration through enhancing its chemical stability while maintaining or improving anticonvulsant potency.

In our first approach, the ortho liable $-NH_2$ group neighboring the carbamate functionality was removed to improve chemical stability. The effects of the deaminated analogues (**L1-1** to **L1-8**) bearing various N-acyl groups on Kv7.2 currents were assessed by using a standard whole-cell recording in CHO cells; the results are summarized in Table 1. Compared with P-RTG, compound **L1-2** without the ortho $-NH_2$ group displayed much reduced potency, with the values of -7.26 ± 2.50 and 1.99 ± 0.37 for $\Delta V_{1/2}$ (mV) and I/I_0, respectively. The carbamate chain replacement from ethyl to isobutyl (**L1-3**), *tert*-butyl (**L1-4**), and allyl (**L1-5**) led to further reduced potencies as indicated by lower ratios of I/I_0. Compound **L1-7** with a hydrophobic benzyl chain displayed much better potency than **L1-6** bearing a hydrophilic glycerol-derived chain with a more left value of $\Delta V_{1/2}$ (mV). By contrast, methyl carbamate, **L1-1** (**CF312**) displayed the best potency among these analogues (**L1-1** to **L1-8**) with values of -24.21 ± 2.35 and 3.27 ± 0.10 for $\Delta V_{1/2}$ (mV) and I/I_0, respectively. It is worth noting that the corresponding acetyl amide analogue **L1-8** with the absence of only one oxygen atom displayed much reduced potency compared with **CF312**. Here, the lack of potency of short-chain amides missing the ortho $-NH_2$ group is consistent with the report by Ostacolo et al. that longer and flexible hydrophobic chain amides more readily interact with a possible whole, large, and hydrophobic pocket on Kv7.2.[32] We assume that methyl carbamate, instead of ethyl carbamate existing in both RTG and P-RTG, is more compatible with the removal of the neighboring $-NH_2$ substituent when incorporating a propargyl group. Therefore, further methyl carbamate analogues were examined in our subsequent work.

The pharmacokinetic parameters of compound **CF312** (30 mg/kg, p.o.) were then assessed in KM mice. Compared to RTG, an inverted brain-to-blood distribution was observed, with C_{max} values of 2197 ng/mL and 4421 ng/g and AUC_{0-t} values of 1865 ng·h/mL and 3565 ng·h/g for the blood and brain, respectively. The brain exposure of **CF312** is 1.9 times greater than its blood exposure, and this is in accordance with the result of P-RTG whose ratio of brain-to-blood exposure is 2.3. This inverted brain-to-blood drug distribution probably resulted from its increased lipophilicity after introducing a propargyl group as reported in our previous work.[41]

The *in vivo* anticonvulsant effects of **CF312** (30 mg/kg, p.o.) were evaluated in the MES mouse model and subcutaneous

https://doi.org/10.1021/acs.jmedchem.0c02252
J. Med. Chem. 2021, 64, 5816−5837

Scheme 3. Synthesis of Deaminated Analogues of P-RTG (L3-1 to L3-13) with a Variety of Substituents on the Right Benzene Ring

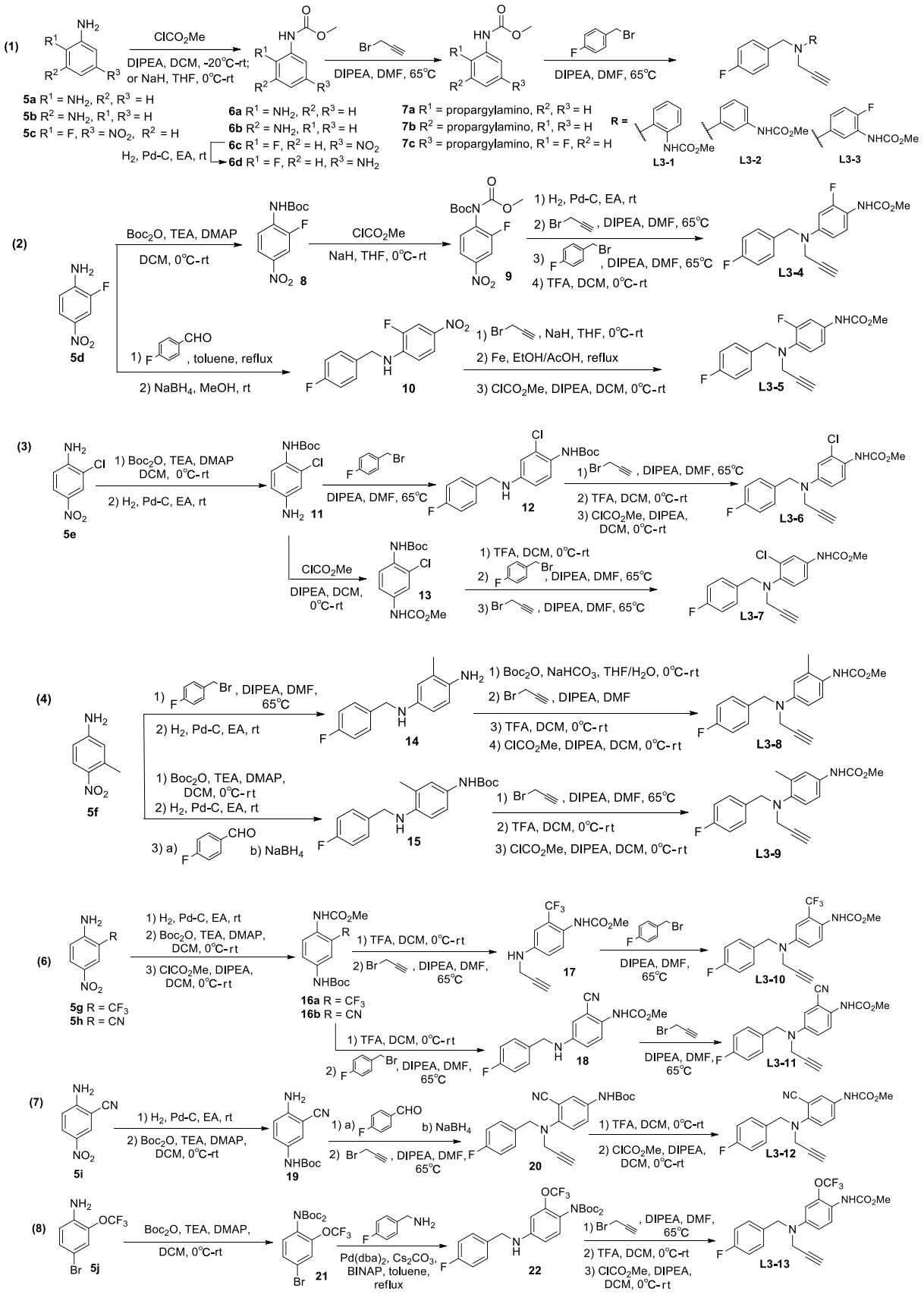

https://doi.org/10.1021/acs.jmedchem.0c02252
J. Med. Chem. 2021, 64, 5816−5837

Scheme 4. Synthesis of Deaminated Analogues of P-RTG (L3-14 and L3-15) with Two Methyl Substituents on the Right Benzene Ring

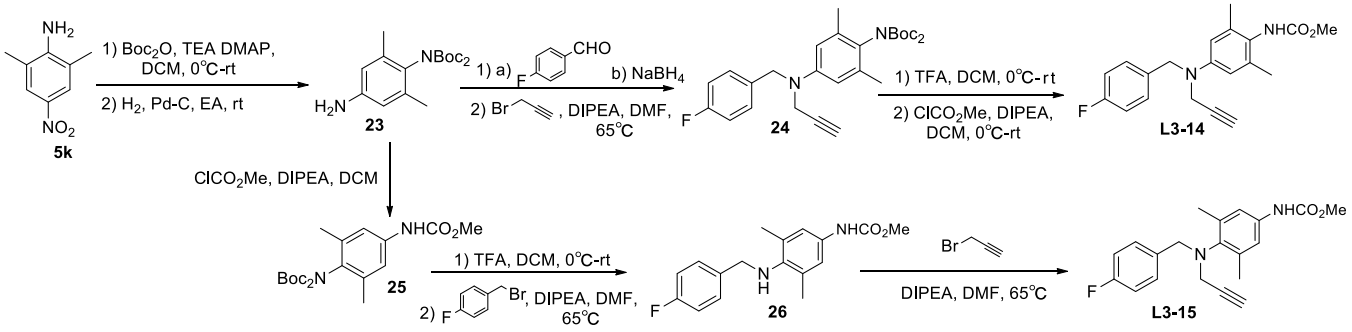

Table 1. Electrophysiological Potencies of RTG, P-RTG, and Deaminated Analogues (L1-1 to L1-8)[a]

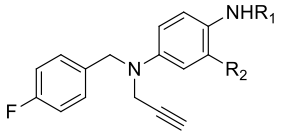

Compound	R^1	R^2	$\Delta V_{1/2}$ (mV)[b]	I/I_0 [c]	N
RTG		NH_2	-33.20±1.00	2.60±0.10	4
P-RTG		NH_2	-47.9±3.50	1.53±0.15	3
L1-1 (CF312)		H	-24.21±2.35	3.27±0.10	3
L1-2		H	-7.26±2.50	1.99±0.37	3
L1-3	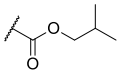	H	-14.32±3.30	1.23±0.08	4
L1-4		H	-19.41±2.23	1.05±0.10	3
L1-5	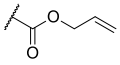	H	-14.46±4.00	1.01±0.03	2
L1-6	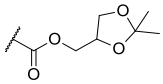	H	-3.95±3.59	2.11±0.03	3
L1-7	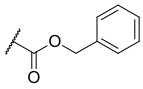	H	-11.52±2.00	2.09±0.25	3
L1-8		H	-6.09±2.45	1.80±0.16	3

[a]All values are expressed as mean ± SEM. [b]The shift of half voltage of maximal activation after administration of 10 μM compound. [c]The amplitude change of outward current: I_0, amplitude of the outward current without the compound; I, amplitude of the outward current with the compound; I/I_0, effect of 10 μM compound on the amplitude of the outward current of KCNQ2 channels.

pentylenetetrazol (sc-PTZ, 85 mg/kg) seizure mouse model. Given orally 1 h prior to the test, **CF312** protected 50% of KM mice from tonic-clonic seizures in the MES test, and 60% of KM mice from clonic seizures in the sc-PTZ test, and the protection of RTG (30 mg/kg, p.o.) against seizures in the MES and sc-PTZ test was 60% and 50%, respectively. Demonstrating that **CF312** maintained considerable efficacy *in vitro* and *in vivo*, our data suggest that the deletion of the ortho $-NH_2$ group is feasible as a result of enhanced tolerance against structural modifications upon incorporating a propargyl group.

CF312, different from other deaminated P-RTG analogues, maintained considerable *in vitro* and *in vivo* potencies. We next undertook a scanning of substituents on the left benzene ring with the right part of the **CF312** structure remaining unchanged. We synthesized a series of **CF312** analogues bearing various substituents at different positions on the left benzene ring. The test results of their electrophysiological potencies are summarized in Table 2.

https://doi.org/10.1021/acs.jmedchem.0c02252
J. Med. Chem. 2021, 64, 5816−5837

Table 2. Electrophysiological Potencies of CF312 Analogues (L2-1 to L2-8) with a Variety of Substituents on the Left Benzene Ring[a]

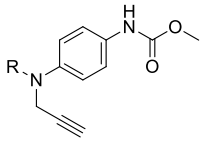

Compound	R	$\Delta V_{1/2}$ (mV)[b]	I/I_0[c]	N
L2-1		-7.60±1.90	2.31±0.36	3
L2-2		-21.10±1.90	2.33±0.17	3
L2-3	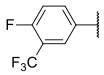	-15.60±1.10	1.33±0.02	3
L2-4	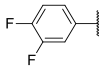	-14.90±2.70	2.52±0.23	3
L2-5		-16.50±2.40	2.29±0.38	3
L2-6	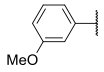	-12.50±3.20	2.72±0.22	5
L2-7	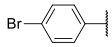	-25.15±1.33	3.75±0.63	5
L2-8	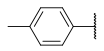	-5.77±1.94	1.05±0.07	3

[a]All values are expressed as mean ± SEM. [b]The shift of the half voltage of maximal activation after administration of 10 μM compound. [c]The amplitude change of the outward current: I_0, amplitude of the outward current without the compound; I, amplitude of the outward current with the compound; I/I_0, effect of 10 μM compound on the amplitude of the outward current of KCNQ2 channels.

The results showed that electrophysiological potencies were very susceptible to substituents on the left benzene ring for reasons of both electronic properties and substitution position. *p*-Fluoro substitution was more beneficial for potency than the respective *o*- and *m*-fluoro counterparts (**L2-1** and **L2-2**). Its *m*-fluoro analogue **L2-2** displayed almost the same level of the left shift value as **CF312** (−21.10 ± 1.90 *vs* −24.21 ± 2.35, $\Delta V_{1/2}$, mV), yet it had a lower activation amplitude (2.33 ± 0.17 *vs* 3.27 ± 0.10, I/I_0). Further introduction of an electron-withdrawing group adjacent to the *p*-fluoro group led to much reduced potency, as illustrated by compounds **L2-3** and **L2-4**, in which a trifluoromethyl group and another fluoro substituent were introduced, respectively. Compared with compounds **L2-2** and **CF312**, the substitution of an electron-donating group (e.g., a methoxy group in **L2-6** and a methyl group in **L2-8**) was detrimental for potency. Interestingly, the *p*-bromo-substituted analogue **L2-7** displayed the same level of potency as **CF312** with values of −25.15 ± 1.33 and 3.75 ± 0.63 for $\Delta V_{1/2}$ (mV) and I/I_0, respectively. In our subsequent work, we maintained *p*-fluoro substitution on the left benzene ring as in **CF312** due to the proved *in vivo* efficacy of **CF312**.

Guided by the results of structure scanning of the carbamate functionality on the right benzene ring and substituents on the left benzene ring, we focused further work on the positions of methyl carbamate functionality and substituents on the right benzene ring. We synthesized and examined a series of methyl carbamate analogues together with a variety of substituents on the right benzene ring; the test results are summarized in Table 3. In contrast to **CF312**, in which the carbamate group takes a para-position, the meta-analogue **L3-2** displayed much reduced potency and the ortho-analogue **L3-1** lost potency completely. These results indicated that a *para*-substituted methyl carbamate functionality on the right benzene ring was critical for maintaining potency. Therefore, a series of **CF312** derivatives with a variety of substituents on the right benzene ring were further examined (Table 3).

The replacement of H atoms with F atoms is a common strategy to modify the structures of many biologically active molecules due to additional beneficial effects of fluoro substitution. In the case of compound **L3-3**, a considerable improvement in potency was observed after introducing a fluoro substituent adjacent to the meta-carbamate functionality in **L3-2**. This result prompted us to further examine the influence of fluoro substitution in **CF312** with a para-carbamate functionality. Unfortunately, **L3-4** displayed no improvement in potency; by contrast, compound **L3-5** showed considerable reduction in potency. Meanwhile, most other **CF312** derivatives, **L3-6**, **L3-7**, **L3-9**, and **L3-10** to **L3-13**, demonstrated much reduced potency, regardless of the electronic nature or the position of these substitutes on the right benzene ring. A surprising exception to this was compound **L3-8**, which had a methyl substituent adjacent to the para-methyl carbamate group and displayed much enhanced potency, with values of −23.28 ± 1.37 and 4.80 ± 0.73 for $\Delta V_{1/2}$ (mV) and I/I_0, respectively. Compared to compound **L3-9** with almost loss of potency, compound **L3-8** displaying notable potency enhancement is impressive. Because the meta-methyl substitution is not beneficial for potency, it is rational to assume that the position of the methyl substitute is responsible for the difference of the observed contrasting potency. We speculate that the huge potency discrepancy between compounds **L3-8** and **L3-9** probably arise from their different conformations rendered by ortho-methyl substitution, which imposes a torsion along the C−N bond due to the increase of steric crowding on the phenyl ring near the carbamate motif. This twisted conformation in which the carbonyl rotates out the plane of the phenyl ring probably favors target binding. Constrained conformation resulting from ortho-methyl substituents also occurs in lidocaine salts where the amide and the phenyl rings are rotated to between 66 and 71° depending on its salt.[42] This is also in accordance with the conformation study on 2,6-dimethyl-acetanilide where the amide and the phenyl ring are rotated to 62.50° based on its X-ray crystallography.[43] Besides, additional possible interactions of ortho-methyl groups with surrounding residues in the large and hydrophobic pockets on $K_V7.2$, to some extent, may also contribute to the advantage of ortho-methyl substitution.

Di-ortho-methyl-substituted anilines are well-established building blocks in Kv7 activators. Similar motifs with one or two ortho-methyl-substituted anilines also occur in many CNS drugs such as some anesthetics, as shown in Figure 2.[44] With this in mind, we next synthesized and examined **L3-14** and **L3-15**, two **CF312** analogues with di-methyl groups on different positions. Compound **L3-14** (**HN37**, pynegabine), with two methyl groups neighboring the carbamate group, showed the best potency among our compounds with values of −38.52 ± 1.67 and 4.75 ± 1.29 for $\Delta V_{1/2}$ (mV) and I/I_0, respectively. By

https://doi.org/10.1021/acs.jmedchem.0c02252
J. Med. Chem. 2021, 64, 5816−5837

Table 3. Electrophysiological Potencies of CF312 Analogues (L3-1 to L3-15) with a Methyl Carbamate Functionality Taking Different Positions and Various Substituents on the Right Benzene Ring[a]

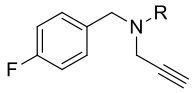

Compound	R	$\Delta V_{1/2}$ (mV)[b]	I/I_0[c]	N
L3-1	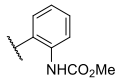	NA[d]	0.95±0.07	3
L3-2	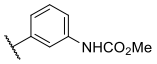	3.60±2.20	1.65±0.07	3
L3-3	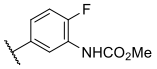	-18.70±2.60	2.75±0.31	3
L3-4	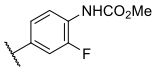	-22.00±1.50	2.09±0.31	3
L3-5	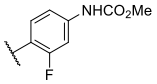	-9.06±0.15	1.39±0.12	3
L3-6	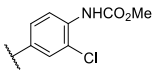	-7.06±1.50	1.09±0.06	3
L3-7	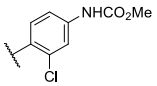	-2.06±0.05	1.19±0.02	3
L3-8	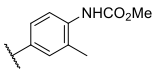	-23.28±1.37	4.80±0.73	3
L3-9	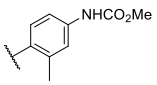	-3.42±1.54	1.40±0.04	3
L3-10	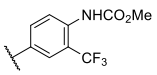	-10.40±2.00	1.42±0.10	3
L3-11	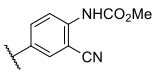	-5.10±0.90	0.52±0.01	3
L3-12	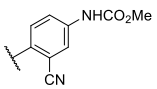	-9.62±3.07	1.94±0.09	3
L3-13	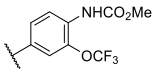	-13.20±1.50	1.24±0.16	3
L3-14 (HN37)	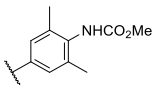	-38.52±1.67	4.75±1.29	3
L3-15	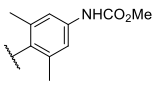	13.47±2.13	0.72±0.05	3

[a]All values are expressed as mean ± SEM. [b]The shift of the half voltage of maximal activation after administration of 10 μM compound. [c]The amplitude change of the outward current: I_0, amplitude of the outward current without the compound; I, amplitude of the outward current with the compound; I/I_0, effect of 10 μM compound on the amplitude of the outward current of KCNQ2 channels. [d]Left shift value was not tested due to its very weak activating potency.

contrast, compound **L3-15**, with two methyl groups on meta-positions, lost potency with an I/I_0 value of 0.72 ± 0.05.

Chemical Stability Evaluations. According to the chemistry reviews, RTG is a nonhygroscopic, white to slightly colored powder. Although pure RTG was reported to be a colorless compound, its crude product was intensively colored and changed quickly from red to dark violet. The darkening of the active substance may be observed when RTG is exposed to light. These indicate that some quinone diimine species could be involved when RTG is exposed to air or light. Actually, two dimeric impurities have been identified as RTG dimers which were probably produced during the later work up procedures or storage.[23] Recently, pigmented dimers of both RTG and its N-acetyl metabolite NAMR were identified by the *in vivo*

https://doi.org/10.1021/acs.jmedchem.0c02252
J. Med. Chem. 2021, 64, 5816−5837

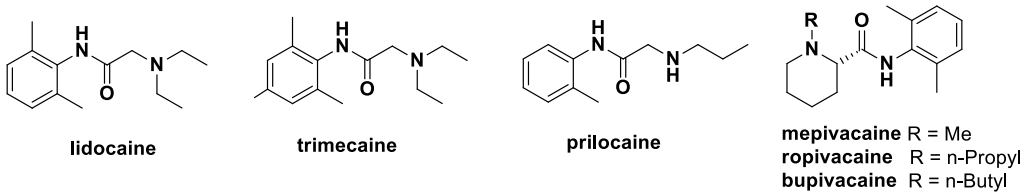

Figure 2. Some anesthetics containing similar motifs with one or two methyl-substituted anilines.

Table 4. Pharmacokinetic Parameters of HN37 in KM Mice

dose		T_{max}[a]	C_{max}[b]	AUC_{0-t}[c]	$t_{1/2}$[d]	CL[e]	V_{ss}[f]	F[g]	ratio of AUC_{0-t}
mg/kg	sample	(h)	(ng/mL)	(ng·h/mL)	(h)	L/h/kg	L/kg	%	brain/plasma
5 (p.o)	plasma	0.25	134	321	1.95			24.2	2.23
	brain	0.25	263	716	1.95				
2 (i.v)	plasma			531	0.80	3.68	2.89		

[a]Time of maximum concentration. [b]Maximum observed plasma concentration. [c]Area under the plasma concentration−time curve from time zero to the last measurable concentrations calculated by the trapezoidal method. [d]Half-life. [e]Clearance. [f]Steady-state distribution volume. [g]Bioavailability.

study, further suggesting the linkage between discoloration and RTG's chemical structure vulnerability.[21] Though RTG's NDA stability packaging includes long-term stability data of 18 months and accelerated data of 6 months, an expiration period of only 15 months for all of its tablet strengths can be supported.

Due to the removal of the liable $-NH_2$ group, compound **HN37** exhibited satisfactory stability with or without packaging when exposed to a high temperature (60 °C), high humidity (25 °C, RH 92.5%), and strong light (5500 Lx). Further stability data include accelerated data stability of 6 months (40 ± 2 °C, RH 75 ± 5%) and long-term stability data up to 36 months (25 ± 2 °C, RH 60 ± 10%). So far, an ongoing drug product stability study can support an expiration period of 36 months for **HN37** tablets with strengths of 5 and 20 mg, which is a much longer shelf life than RTG.

Pharmacokinetic Study. The pharmacokinetic properties of **HN37** were then examined in KM mice; the results are summarized in Table 4. **HN37** was quickly absorbed showing a T_{max} of 0.25 h in both the blood and brain, and C_{max} values of 134 and 263 ng/mL, respectively. The blood and brain distributions were observed with AUC_{0-t} of 321 and 716 ng·h/mL for the plasma and brain, respectively. The calculated ratio of the brain to blood exposure for **HN37** was 2.23 times, a sharp contrast to a ratio of 0.16 for RTG.[41] This inverted brain-to-blood distribution for **HN37** likely arises from its increased lipophilicity due to the installation of one propargyl group and two methyl substituents. Without regard to the brain distribution, **HN37** showed a moderate bioavailability (24.2%, F) in KM mice.

Further pharmacokinetic studies of **HN37** are carried out in SD rats in a dose-escalating manner (2, 6 and 20 mg/kg, p.o.), and the results are summarized in Table 5. In rats, **HN37** reached its highest concentration after 0.50, 0.67, and 3.67 h, with C_{max} values of 88.2, 264, and 323 ng/mL at the oral dose of 2, 6, and 20 mg/kg, respectively. Almost in proportion to the dosages, the corresponding AUC_{0-t} values in the blood were 247, 1130, and 1921 ng·h/mL, respectively. In another set of experiments, the pharmacokinetic parameters of **HN37** (6 mg/kg, p.o.) in both the blood and brain were examined at the same time. **HN37** reached its highest concentration in both the brain and blood at 0.25 h after oral administration, and AUC_{0-t} values were found to be 1524 and 533 ng·h/mL, respectively. In accordance with the results in KM mice, **HN37** tended to distribute in brain with the calculated ratio of brain to blood exposure as 2.86 in rats.

Table 5. Pharmacokinetic Parameters of HN37 in SD Rats via Oral Administration

dose (mg/kg)		T_{max}[a] (h)	C_{max}[b] (ng/mL)	AUC_{0-t}[c] (ng·h/mL)	$t_{1/2}$[d] (h)
2		0.50	88.2	247	1.72
6		0.67	264	1130	2.36
20		3.67	323	1921	
6	brain	0.25	578	1524	ratio of AUC_{0-t} brain/plasma
	blood	0.25	162	533	2.86

[a]Time of maximum concentration. [b]Maximum observed plasma concentration. [c]Area under the plasma concentration−time curve from time zero to the last measurable concentrations calculated by the trapezoidal method. [d]Half-life.

The metabolic stability of **HN37** toward human, monkey, dog, rat, and mice liver microsomes is examined, and the results are showed in Table 6. According to these data, **HN37** belongs to a class of high clearance with the highest clearance rate in mice among these species. Its CL_{int} in mice is up to 438 mL/min/kg together with a short $T_{1/2}$ of 12.5 min, which may explain its high clearance in mice.

Table 6. Metabolic Stability Data of HN37 toward Human, Monkey, Dog, Rat, and Mice Liver Microsomes

liver microsomes	$T_{1/2}$ (min)	CL_{int} (mL/min/kg)
human	27.7	62.7
monkey	18.1	112
dog	35.5	97.2
rat	23.7	105
mice	12.5	438

A major cytochrome P450s inhibition assay was carried out using specific probe substrates in the presence of human liver microsomes and the results are summarized in Table S1. Data showed that **HN37** at a concentration ranging from 0.10 to 50.0 μM had no significant inhibition (<25% in all cases) toward main human CYP isoforms, including CYP1A2, CYP2B6, CYP2C8, CYP2C9, CYP2C19, CYP2D6, and

https://doi.org/10.1021/acs.jmedchem.0c02252
J. Med. Chem. 2021, 64, 5816−5837

Table 7. Subtype Selectivity of HN37 and RTG[a]

	compound			
	HN37		RTG	
KCNQ subtype	$\Delta V_{1/2}$ (mV)[b]	I/I_0[c]	$\Delta V_{1/2}$ (mV)[b]	I/I_0[c]
KCNQ1	−5.47 ± 2.86	0.99 ± 0.04	−8.03 ± 2.59	1.01 ± 0.05
KCNQ2	−35.60 ± 4.14	3.40 ± 0.26	−46.10 ± 3.66	1.79 ± 0.11
KCNQ3 (A278T)	−43.11 ± 4.42	2.10 ± 0.29	−46.83 ± 5.87	2.46 ± 0.20
KCNQ2/KCNQ3	−60.21 ± 4.42	2.77 ± 0.18	−34.32 ± 4.07	1.97 ± 0.06
KCNQ4	−56.63 ± 9.76	3.76 ± 0.56	−34.09 ± 6.90	2.85 ± 0.35
KCNQ5	−9.03 ± 1.29	3.14 ± 0.46	0.09 ± 8.61	3.04 ± 0.32

[a]All values are expressed as mean ± SEM (n = 3−5). [b]The shift of the half voltage of maximal activation after administration of 0.1 μM **HN37** or 10 μM RTG. [c]The amplitude change of the outward current: I_0, amplitude of the outward current without the compound; I, amplitude of the outward current with the compound; I/I_0, effect of 0.1 μM HN37 or 10 μM RTG on the amplitude of the outward current of KCNQ channels.

CYP3A4. In view of the potential metabolic liability of **HN37** due to the propargyl group containing a triple bond, potentials of time-dependent inhibition (TDI) for **HN37** on cytochrome P450s are assessed using human liver microsomes, and the results are summarized in Figure S1; TDI test results showed that **HN37** was not a time-dependent inhibitor toward CYP2C9, CYP2C19, CYP2D6, CYP3A4 (midazolam 1′-hydroxylation), and CYP3A4 (testosterone 6β-hydroxylation), with both $IC_{50NADPH^+}$ and $IC_{50NADPH^-}$ above 50 μM and the ratio of $IC_{50NADPH^-}/IC_{50NADPH^+}$ less than 1.5; **HN37** displayed time-dependent inhibition toward CYP1A2 ($IC_{50NADPH^+}$ = 2.53, $IC_{50NADPH^-}$ = 142 μM), CYP2B6 ($IC_{50NADPH^+}$ = 5.76 μM, $IC_{50NADPH^-}$ = 141 μM), and CYP2C8 ($IC_{50NADPH^+}$ = 35.2 μM, $IC_{50NADPH^-}$ = 225 μM), where the ratio of $IC_{50NADPH^-}/IC_{50NADPH^+}$ in each case was higher than 1.5. The potential of **HN37** to cause time-dependent inhibition of CYP1A2, CYP2B6, and CYP2C8 will be further evaluated in its clinical study.

We next carried out a series of pre-clinical experiments, and the results are summarized below.

Selectivity Among KCNQ Channels. Previous studies have shown that RTG mainly serves as a pan-agonist at Kv7.2−Kv7.5 channels, particularly the KCNQ2/3 heterotetramer.[45] To determine the subtype selectivity and agonist potency of HN37 among KCNQ channels, the amplitude changes of the outward current (I/I_0) and the shift of the half voltage of maximal activation ($\Delta V_{1/2}$) were measured using patch-clamp assays. CHO cells transiently transfected with hKCNQ1, rKCNQ2, rKCNQ3* (an expression-optimized KCNQ3-A278T mutant at the pore region that ensures robust currents to ascertain the observation),[46−48] hKCNQ4, and hKCNQ5 were used for the recording in this study. As shown in Table 7, after 0.1 μM **HN37** application, the outward currents were potentiated in all the tested KCNQ isoforms except KCNQ1 (cardiac isoform). The voltage-dependent activation curves showed left shift effects in neuronal isoforms, and the most obvious effect was KCNQ2/KCNQ3 ($V_{1/2}$ with a left-shift of 60.21 ± 4.42 mV). These results indicate that compound **HN37** is a potent neuronal Kv7 activator with a subtype selectivity similar to RTG.

Given that the neuronal M-current, mainly mediated by KCNQ2/KCNQ3 and KCNQ2 channels, plays an important role in the regulation of neuronal excitability,[49,50] we further examined the dose-effect relationship of compound **HN37** and RTG on KCNQ2/KCNQ3 and KCNQ2 channels. The median effective concentration (EC_{50}) was determined by a dose−response curve analysis, the results are shown in Figure 3. For KCNQ2 channels, the EC_{50} of **HN37** was 36.98 ± 6.17 nM, which is 55-fold more potent than that of RTG (2.04 ± 0.25 μM) (Figure 3A). For KCNQ2/KCNQ3 channels, **HN37** had an EC_{50} value of 33.07 ± 4.36 nM, showing a nearly 125-fold increased potency compared to RTG (4.15 ± 0.54 μM) (Figure 3B). The above results suggest that **HN37** has a greater ability to dampen neuronal excitability than RTG.

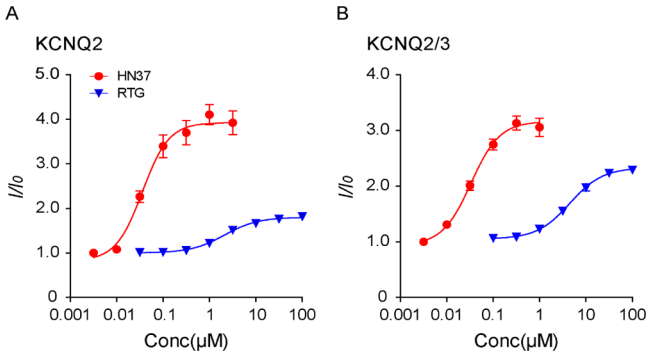

Figure 3. Effects of HN37 and RTG on KCNQ2 (A) and KCNQ2/3 (B). Data are expressed as mean ± SEM (n = 4−6 at each concentration).

Anticonvulsant Efficacy. To test and evaluate the anticonvulsant activities of compound **HN37**, the efficacy was tested in a range of seizure models according to the Epilepsy Therapy Screening Program (ETSP) sponsored by the National Institute of Neurological Disorders and Stroke (NINDS). ETSP is the new name for the Anticonvulsant Screening Program (ASP), which has tested tens of thousands of compounds from dozens of countries[51] and has made an important contribution to the identification and/or characterization of several FDA-approved drugs for epilepsy for over 40 years, including topiramate, lacosamide, felbamate, and retigabine.[51,52] The current work flow for the ETSP focuses on compound evaluation by using pharmacoresistant models and begins with the assessment in two acute seizure models, the maximal electroshock (MES) seizure test and the 6 Hz seizure test of pharmacoresistant epilepsy. The MES test is considered as a predictive model for generalized tonic−clonic seizures, and it may also predict antiepileptic drugs with efficacy against partial seizures.[53,54] The 6 Hz psychomotor seizure is similar to human limbic epilepsy and shows resistance to numerous current AEDs especially under the high stimulus intensity (44 mA).[52,55] These two seizure models were used in this study. In addition, another classic seizure model, the subcutaneous pentylenetetrazol (sc-PTZ) seizure

https://doi.org/10.1021/acs.jmedchem.0c02252
J. Med. Chem. 2021, 64, 5816−5837

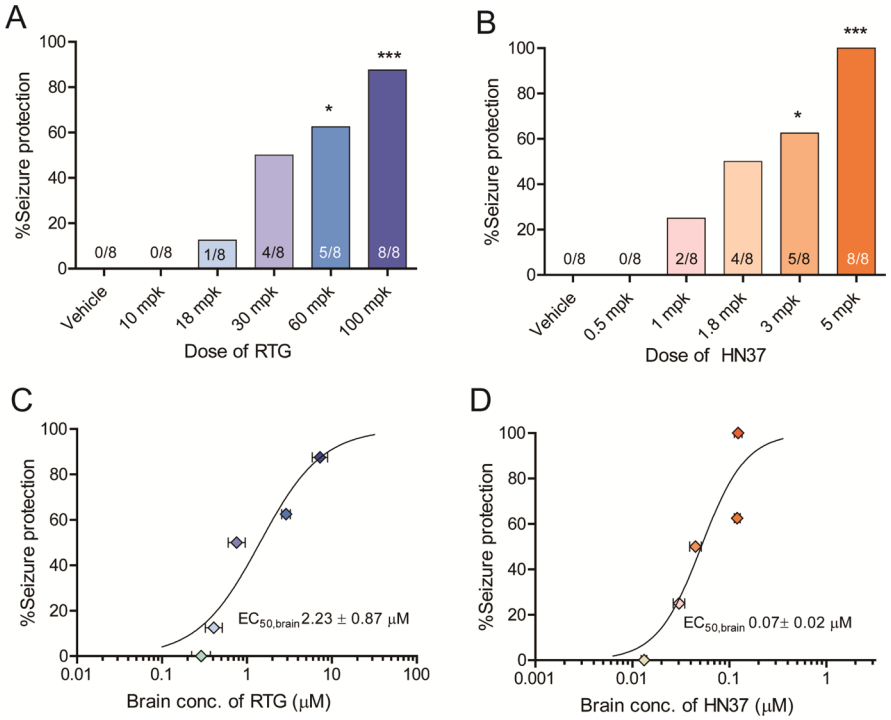

Figure 4. (A,B) Effects of HN37 and RTG in the MES seizure model in KM mice. % seizure protection is a percentage of animals not displaying hindlimb tonic extension. The data for each dose are presented as N/T (N = number of animals protected, T = number of animals tested) and stated in each bar. Fisher's exact probability test was used for statistical analysis: $^{*}p < 0.05$, $^{**}p < 0.01$, $^{***}p < 0.001$ *vs* vehicle. (C,D) Concentration−response curves of HN37 and RTG for seizure protection in the MES seizure model. Data are expressed as mean brain concentration ± SEM. The EC_{50} values are calculated by nonlinear regression using GraphPad Prism 5.

Table 8. Mean Brain or Plasma Concentration of HN37 and RTG in MES and Rotarod Tests in KM Mice

compound	test	brain conc. EC_{50} or TC_{50} (μM)[a]	plasma conc. EC_{50} or TC_{50} (μM)[a]	brain/plasma conc. ratio	brain conc. TC_{50}/EC_{50} ratio
HN37	MES	0.07 ± 0.02	0.05 ± 0.01	1.4	N/A[b]
RTG		2.23 ± 0.87	20.04 ± 6.73	0.11	N/A[b]
HN37	rotarod	3.47 ± 0.26	1.83 ± 0.26	1.9	49.6
RTG		27.32 ± 12.84	141.33 ± 64.48	0.19	12.3

[a]Values are expressed as mean ± SEM; EC_{50} or TC_{50} values are determined by nonlinear regression using GraphPad Prism 5. [b]Not Applicable.

test, was also used to detect the anticonvulsant efficacy against clonic seizures.[54]

First, the time effect of compound **HN37** was tested in the MES seizure model by oral gavage administration at a dose of 2.5 mg/kg in KM mice, and the animals, whether displaying hindlimb tonic extension, were observed at 0.25, 0.5, 1, and 2 h after administration. Compound **HN37** showed 40−80% constant seizure protection from 0.25 to 2 h and exhibited its peak effect at 1 h (Table S2). Then, on the basis of the above results, dose−response quantification studies were further carried out at 1 h to elucidate the median effective dose (ED_{50}) in the MES test. Subsequently, the median neurotoxic dose (TD_{50}) at a peak time of 1 h was determined using the rotarod test. After completion of both tests, animals were euthanized immediately, and plasma and brain samples were collected to detect the levels of compound **HN37** and RTG.

In the MES test, compound RTG (10−100 mg/kg, p.o.) showed a dose-dependent efficacy against seizures, and the seizure protections were 62.5 and 87.5% at the 60 and 100 mg/kg doses, respectively, with statistically significant differences from the vehicle (Figure 4A). Compound **HN37** displayed improved efficacy compared to RTG after 1 h oral administration, and the significant effects were observed at the low doses of 3 and 5 mg/kg, with seizure protections of 62.5 and 100%, respectively (Figure 4B). The ED_{50} value of **HN37** calculated by the dose−response curve in this test was 1.9 mg/kg, which was much lower than that of RTG (38.6 mg/kg). Further PK studies showed that RTG achieved a maximal brain concentration of 8.29 μM and a maximal plasma concentration of 40.85 μM at the highest dose of 100 mg/kg, and the $EC_{50,brain}$ value of 2.23 ± 0.87 μM was calculated by a concentration−response curve, with a corresponding $EC_{50,plasma}$ value of 20.04 ± 6.73 μM (Figure 4C, Table 8). The average brain/plasma concentration ratio (B/P) for RTG was 0.11, which was consistent with the previous study.[42] The maximal brain and plasma concentration of **HN37** was 0.12 and 0.11 μM at 5 mg/kg, respectively. The concentration−response curves showed that the $EC_{50,brain}$ and the corresponding $EC_{50,plasma}$ values for **HN37** were 0.07 ± 0.02 and 0.05 ± 0.01 μM, respectively, and the average B/P was 1.4, much higher than RTG (Figure 4D, Table 8).

Meanwhile, the neurotoxicity effects of compound **HN37** and RTG were observed in the rotarod test under the same experimental conditions. After 1 h oral administration, compound RTG produced a dose-dependent increase in the

https://doi.org/10.1021/acs.jmedchem.0c02252
J. Med. Chem. 2021, 64, 5816−5837

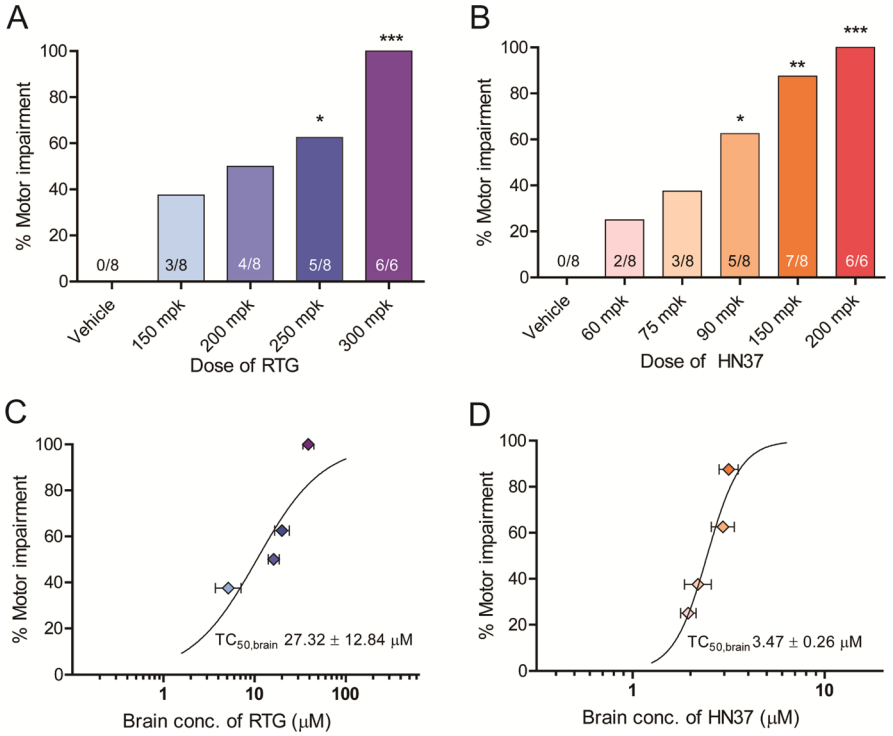

Figure 5. (A,B) Effects of HN37 and RTG in the rotarod test in KM mice. % motor impairment is a percentage of animals falling off the rotating rod. The data for each dose are presented as N/T (N = number of animals exhibiting toxicity, T = number of animals tested) and stated in each bar. Fisher's exact probability test was used for statistical analysis: $*p < 0.05$, $**p < 0.01$, $***p < 0.001$ *vs* vehicle. (C,D) Concentration−response curves of HN37 and RTG for motor impairment in the rotarod test. Data are expressed as mean brain concentration ± SEM. The TC_{50} values are calculated by nonlinear regression using GraphPad Prism 5.

Table 9. Anticonvulsant Effects of HN37 and Three Reference Drugs (p.o.) in the KM Mouse-Induced MES and PTZ Seizure Models[a]

compound	time of test (h)	MES ED_{50} (mg/kg)[b]	PTZ ED_{50} (mg/kg)[c]	TD_{50} (mg/kg)[d]
HN37	1.0	1.9 (1.3−2.8)	9.8 (4.5−21.3)	82.0 (74.8−89.8)
RTG[e]	1.0	38.6 (25.1−59.3)	>56	187.7 (116.7−301.9)
TPM[e]	1.0	35.5 (23.3−54.1)	>200	379.2 (287.6−499.9)
LEV[e]	1.0	>500	>500	>500

[a]Values in parentheses are 95% confidence intervals determined by nonlinear regression using GraphPad Prism 5. [b]ED_{50} (MES—maximal electroshock seizure model). [c]ED_{50} (sc-PTZ—pentylenetetrazol seizure model). [d]TD_{50} (NT—acute neurological toxicity determined in the rotarod test). [e]Reference AEDs: retigabine (RTG), levetiracetam (LEV), and topiramate (TPM) tested under the same conditions.

motor impairment and had significant effects on the ability to remain on the rotarod at the 250 and 300 mg/kg, with 62.5 and 100% motor impairment rate, respectively (Figure 5A). Compound **HN37** also showed a dose-dependent injury to the motor behavior, and it exhibited significant effects on motor coordination at the doses of 90, 150, and 200 mg/kg with motor impairment rates of 62.5, 87.5, and 100%, respectively (Figure 5B). Both **HN37** and RTG did not produce obvious effects on motor coordination at 60 mg/kg, and the TD_{50} values determined by dose−response curves were 82.0 and 187.7 mg/kg, respectively. Further PK studies showed that RTG had a maximal brain concentration of 41.62 and 134.89 μM in the plasma at the highest dose of 300 mg/kg. The concentration−response curves demonstrated that the $TC_{50,brain}$ and the corresponding $TC_{50,plasma}$ values of RTG were 27.32 ± 12.84 and 141.33 ± 64.48 μM, respectively (Figure 5C, Table 8), and the average B/P was 0.19, consistent with the results in the MES test and previous study.[42] Both $TC_{50,brain}$ and the corresponding $TC_{50,plasma}$ of **HN37** were also calculated from the concentration−response curves, and the values were 3.47 ± 0.26 and 1.83 ± 0.26 μM, respectively (Figure 5D, Table 8). **HN37** had a much higher average B/P ratio (1.9) than that of RTG, this result was consistent with the results in the MES test and PK studies in mice. To better understand the tolerability, the safety margins for **HN37** and RTG based on the brain exposures were calculated, and the $TC_{50,brain}/EC_{50,brain}$ ratio values of **HN37** and RTG were 49.6 and 12.3, respectively (Table 8). The above results suggest that compound **HN37** has a better safety margin than RTG between behavior efficacy and neurotoxicity.

To obtain more data to assess **HN37**'s efficacy against seizures, the anticonvulsive effects and neurotoxicity of reference AEDs, including commonly used drug Levetiracetam (LEV) and Topiramate (TPM), were tested in MES and rotarod tests under the same experimental conditions, and the ED_{50} values were also determined in the sc-PTZ seizure model at the 1 h peak time. The data tested in KM mice are summarized in Table 9. Although LEV was well tolerated in the rotarod test, it did not produce any anticonvulsant effects in MES and PTZ tests; and TPM also showed limited efficacy

https://doi.org/10.1021/acs.jmedchem.0c02252
J. Med. Chem. 2021, 64, 5816−5837

in the PTZ test but had potent anticonvulsant efficacy in the MES test with an ED_{50} value of 35.5 mg/kg. These were in line with those reported in the literature.[56,57] As mentioned earlier, RTG was very effective for tonic seizure but not for clonic seizure even at the highest oral dose of 56 mg/kg in the PTZ test, this might be due to the use of a higher dosage of PTZ (100 mg/kg). Unlike the reference AEDs, compound **HN37** showed a higher efficacy both in MES and PTZ tests, with the ED_{50} values of 1.9 and 9.8 mg/kg, respectively. Notably, the TD_{50}/ED_{50} ratios of **HN37** and RTG (43.2, 4.9) were actually close to the mean $TC_{50,brain}/EC_{50,brain}$ ratios (49.6, 12.3) based on brain exposure, so we think that **HN37** has a better safety margin (8.4-fold in the PTZ test) than that of the other three AEDs in this study.

In addition, the quantification study of the ED_{50} was also examined in the rat MES test. Given orally 0.5 or 1 h prior to testing, the ED_{50} values determined for **HN37** were 2−4-fold more beneficial than that of RTG and were also better than that for TPM (18.7-fold greater) at 1 h (Table S3). These results indicate that compound **HN37** has potent anticonvulsant efficacy in rats.

The 6 Hz psychomotor seizure model is an acute model for drug-resistant epilepsy and is used for the pharmacoresistant drug screen in the ETSP work flow as with the MES seizure model. Therefore, compound HN37 and the reference drugs were also tested in the 6 Hz seizure test in C57BL/6 mice. As shown in Table 10, except TPM, the other two reference drugs

Table 10. Anticonvulsant Effects of HN37 and Three Reference Drugs (p.o.) in the C57BL/6 Mouse-Induced 6 Hz Seizure Model[a]

compound	time of test (h)	6 Hz 32 mA ED_{50} (mg/kg)[b]	6 Hz 44 mA ED_{50} (mg/kg)[b]
HN37	1.0	16.8 (14.7−19.1)	29.9 (23.0−38.8)
RTG[c]	1.0	65.9 (58.6−74.0)	102.5 (91.6−114.8)
TPM[c]	1.0	>500	>500
LEV[c]	1.0	41.5 (17.9−96.1)	376.4 (341.2−415.3)

[a]Values in parentheses are 95% confidence intervals determined by nonlinear regression using GraphPad Prism 5. [b]ED_{50} (6 Hz psychomotor seizure model, 32 mA or 44 mA). [c]Reference AEDs: retigabine (RTG), levetiracetam (LEV), and topiramate (TPM) tested under the same conditions.

LEV and RTG demonstrated potent anticonvulsant effects on the 6 Hz seizure at both 32 and 44 mA stimulus intensities, which was in conformity to the published report.[56,57] Compound **HN37** was also highly effective in the 6 Hz seizure test at both 32 and 44 mA, with ED_{50} values of 16.8 and 29.9 mg/kg, respectively. As the 6 Hz stimulus current increases from 32 to 44 mA, most AEDs lose efficacy and few are only effective at the neurotoxic doses, just like the three reference AEDs in the present study.[53,57] Under the higher stimulus intensity (44 mA), LEV was only effective at very high doses (ED_{50} = 376.4 mg/kg), and RTG produced visible sedative effects at the effective doses of 80 mg/kg and higher in this animal strain. However, **HN37** showed much more efficacy and did not produce obvious motor impairment at the effective doses. Thus, based on the efficacy and tolerability, **HN37** is a promising candidate for epilepsy and has potential for efficacy in clinical pharmacoresistant patients.

CONCLUSIONS

Kv7 channels hold great promise for developing novel AEDs to fulfill unmet clinical demands. Unfortunately, the supply of the first and only launched drug retigabine has been discontinued for commercial reasons due to safety issues such as skin and retina discolorations, although these are unrelated to its mechanism of action. The incorporation of a propargyl group at the N position of the RTG linker opened a new avenue for its structural modifications and optimization, which eventually led to the discovery of **HN37** (compound **L3−14**). **HN37** is a new generation of Kv7 activator that avoids the potential of forming pigmented dimers. Encouraged by its *in vivo* efficacy, PK characteristics, improved safety margin, and satisfactory chemical stability, we have completed its IND application and received approval for clinical study from the National Medical Products Administration (NMPA). The potential of **HN37** to cause time-dependent inhibition of CYP1A2, CYP2B6, and CYP2C8 will be further evaluated during the clinical study, and its first-in-human (FIH) results will be reported in due course.

EXPERIMENTAL SECTION

Synthetic Materials and Methods. Starting materials, reagents, and solvents were purchased from commercial suppliers and used without further purification. Anhydrous toluene, THF, and DCM were obtained from a distillation over a sodium wire or CaH_2. Reactions were carried out with magnetic stirring in round-bottomed flasks unless otherwise noted. Moisture-sensitive reactions were conducted in oven-dried glassware using a freshly distilled solvent under a nitrogen atmosphere with rigid exclusion of moisture. Thin-layer chromatography (TLC) was carried out on pre-coated TLC plates with silica gel HSGF 254. Spots were visualized under UV at 254 nm. Flash chromatography was performed on glass columns packed with silica gel using PE/EA with varying proportions as the mobile phase. ^{1}H NMR and ^{13}C NMR spectra were measured on a Varian Mercury-VX 300, Varian MR 400, AVANCE III 500, or AVANCE III 600 spectrometer using deuterated chloroform ($CDCl_3$) as the solvent. Chemical shifts are expressed in δ (ppm) relative to internal Me_4Si for ^{1}H and ^{13}C NMR. HR-MS were measured on a Micromass Ultra Q-Tof. The purity of all final compounds was ≥95% confirmed by analytical HPLC chromatograms using an Agilent 1200 series LC system equipped with a degasser, a quaternary pump, an auto sampler, a column oven, and a diode array detector. Analytes were separated on a Zorbax SB C18 column (4.6 × 150 mm, 5 μm). Solvent A was 0.1% trifluoroacetic acid in H_2O and solvent B was 100% methanol. Gradient elution: 20% B for 2 min, then 20−80% B from 2 to 20 min, and 80% B was maintained for 5 min, then 80−20% B from 25 to 30 min. All compounds were monitored at 262 nm at room temperature. Flow rate: 1.0 mL/min.

General Procedure A: Reductive Amination Reaction. To a solution of commercially available anilines (1.0 equiv) in toluene was added *p*-fluorobenzaldehyde and catalytic amount *p*-TsOH (0.025 equiv). The resulting mixture was heated to reflux with a Dean−Stark trap until completion. After cooling to room temperature, the mixture was concentrated to dryness in vacuo. The obtained residue was re-dissolved in dioxane/MeOH (4/1, v/v) or MeOH, and solid $NaBH_4$ was added in portions at room temperature. The mixture was allowed to stir until completion, quenched and diluted with water, and extracted with EA. The combined organic phase was washed with brine, dried over anhydrous Na_2SO_4, filtered, and concentrated to dryness in vacuo. Further purification by flash chromatography gave the desired product.

General Procedure B: N-Alkylation Reactions of Anilines. To a solution of anilines in DMF was added proper bromide and DIPEA. The mixture was stirred at 65 °C until completion. After cooling to room temperature, the mixture was diluted with water and extracted with EA. The combined organic phase was washed with water, brine, dried over anhydrous Na_2SO_4, filtered, and concentrated to dryness in

https://doi.org/10.1021/acs.jmedchem.0c02252
J. Med. Chem. 2021, 64, 5816−5837

vacuo. Further purification by flash chromatography gave the desired product.

General Procedure C: Deprotection Reactions of Boc-Protected Anilines. To a stirred solution of Boc-protected anilines in DCM was added TFA dropwise with stirring at 0 °C using an ice-water bath. The mixture was allowed to stir at room temperature until completion. Then, the mixture was concentrated to dryness in vacuo and was used in the next reaction without purification.

General Procedure D: N-Acylation Reactions of Anilines. DIPEA was added to a solution of anilines in dioxane or DCM. After cooling to 0 °C using an ice-water bath, proper acyl chloride was added dropwise. The reaction mixture was stirred at room temperature until completion. Then, the mixture was quenched with water and extracted with EtOAc. The combined organic phase was washed with brine, dried over anhydrous Na_2SO_4, filtered, and concentrated to dryness in vacuo. Further purification by flash chromatography gave the desired product.

General Procedure E: Boc Protection Reactions of Anilines. TEA and DMAP were added to a solution of anilines in DCM. After cooling to 0 °C using an ice-water bath, Boc_2O was added. The mixture was allowed to stir at room temperature until completion. Then, the reaction mixture was poured into water and extracted with EA. The combined organic phase was washed with 1 N HCl, water, brine, dried over anhydrous Na_2SO_4, filtered, and concentrated to dryness in vacuo. Further purification by flash chromatography gave the desired product.

General Procedure F: Nitro Reduction Reactions of Nitro Compounds. *Method A.* Under a nitrogen atmosphere, a catalytic amount of 10% Pd/C was added to a solution of the nitro compound in EA. Then, the reaction atmosphere was changed to hydrogen using a H_2 balloon and the mixture was allowed to stir at room temperature until completion. The mixture was filtered under a nitrogen atmosphere, and the filtrate was concentrated to dryness in vacuo and was used in the next reaction without purification.

Method B. The Fe powder was added to a solution of the nitro compound in EtOH/AcOH (40/1, v/v). The mixture was heated to reflux until completion. After cooling to room temperature, the mixture was filtered, and the filtrate was concentrated in vacuo. The obtained residue was re-dissolved in EA, washed with saturated $NaHCO_3$ aqueous solution, brine, dried over anhydrous Na_2SO_4, filtered, and concentrated to dryness in vacuo. Further purification by flash chromatography gave the desired product.

*tert-Butyl (4-((4-Fluorobenzyl)amino)phenyl)carbamate (**2**).* Following general procedure A, *tert*-butyl (4-aminophenyl)carbamate **1** (2.57 g, 12.3 mol) was condensed with *p*-fluorobenzaldehyde (1.69 g, 13.6 mmol) catalyzed by *p*-TsOH (53 mg, 0.3 mmol) in toluene (50 mL) after reflux for 3 h, followed by reduction by $NaBH_4$ (0.7 g, 18.4 mmol) in dioxane/MeOH (10 mL/2.5 mL) at room temperature for 2 h. Purification by flash chromatography (PE/EA, 6/1, v/v) gave the title compound as a pale yellow solid (3.5 g, 90% over two steps). ^{1}H NMR (300 MHz, $CDCl_3$): δ 7.31 (t, J = 8.4 Hz, 2H), 7.14 (d, J = 8.4 Hz, 2H), 7.01 (t, J = 8.7 Hz, 2H), 6.56 (d, J = 9.0 Hz, 2H), 6.22 (s, 1H), 4.27 (s, 2H), 1.50 (s, 9H).

*tert-Butyl (4-((4-Fluorobenzyl)(prop-2-yn-1-yl)amino)phenyl)carbamate (**L1-4**).* Following general procedure B, compound **1** (316 mg, 1.0 mmol) was reacted with propargyl bromide (102 μL, 1.3 mmol) and DIPEA (383 μL, 2.2 mmol) in DMF (15 mL) at 65 °C for 2 h. Purification by flash chromatography (PE/EA, 8/1, v/v) gave the title compound as a yellow solid (330 mg, 93%). ^{1}H NMR (300 MHz, $CDCl_3$): δ 7.21−7.30 (m, 4H), 7.00 (t, J = 8.4 Hz, 2H), 6.86 (d, J = 9.0 Hz, 2H), 6.32 (s, 1H), 4.42 (s, 2H), 3.92 (d, J = 2.4 Hz, 2H), 2.20 (t, J = 2.4 Hz, 1H), 1.50 (s, 9H); ^{13}C NMR (75 MHz, $CDCl_3$): δ 163.29, 160.86, 153.25, 145.08, 133.99, 130.23, 129.12, 120.61, 115.96, 115.49, 115.28, 80.17, 79.40, 72.47, 54.77, 40.43, 28.38; HRMS (TOF ESI) m/z: calcd for $C_{21}H_{24}FN_2O_2$ $[M + H]^+$, 355.1822; found, 355.1814; HPLC purity: 95.2%.

*Methyl (4-((4-Fluorobenzyl)(prop-2-yn-1-yl)amino)phenyl)carbamate (**L1-1**).* Following general procedure C, compound **L1-4** (150 mg, 0.42 mmol) was deprotected using TFA (0.2 mL) in DCM (2 mL) at room temperature for 2 h; further following General Procedure D, the deprotected intermediate was reacted with methyl chloroformate (40 μL, 0.52 mmol) and DIPEA (146μL, 0.84 mmol) in DCM (2 mL) at room temperature for 2 h. Purification by flash chromatography (PE/EA, 8/1, v/v) gave the title compound **L1-1** as a pale yellow solid (100 mg, 76% over two steps). ^{1}H NMR (300 MHz, $CDCl_3$): δ 7.23−7.28 (m, 4H), 6.99 (t, J = 8.4 Hz, 2H), 6.83 (d, J = 8.7 Hz, 2H), 4.41 (s, 2H), 3.91 (s, 2H), 3.72 (s, 3H), 2.22 (s, 1H); ^{13}C NMR (75 MHz, $CDCl_3$): δ 163.74, 160.49, 145.36, 134.04, 129.15, 120.79, 115.74, 115.62, 115.34, 79.52, 72.68, 54.78, 52.31, 40.37; HRMS (TOF ESI) m/z: calcd for $C_{18}H_{18}FN_2O_2$ $[M + H]^+$, 313.1352; found, 313.1342; HPLC purity: 98.5%.

*Ethyl (4-((4-Fluorobenzyl) (prop-2-yn-1-yl)amino)phenyl)carbamate (**L1-2**).* Following procedures similar to that described for compound **L1-1** gave compound **L1-2** as a yellow solid (73% over two steps). ^{1}H NMR (300 MHz, $CDCl_3$): δ 7.23−7.29 (m, 4H), 7.00 (t, J = 8.4 Hz, 2H), 6.85 (d, J = 9.0 Hz, 2H), 6.59 (s, 1H), 4.42 (s, 2H), 4.18 (q, J = 7.2 Hz, 2H), 3.92 (d, J = 2.1 Hz, 2H), 2.21 (t, J = 2.4 Hz, 1H), 1.28 (t, J = 7.2 Hz, 3H); ^{13}C NMR (75 MHz, $CDCl_3$): δ 163.82, 160.57, 145.40, 134.11, 129.23, 120.87, 115.91, 115.67, 115.39, 79.56, 72.68, 61.19, 54.87, 40.48, 14.74; HRMS (TOF ESI) m/z: calcd for $C_{19}H_{20}FN_2O_2$ $[M + H]^+$, 327.1509; found, 327.1501; HPLC purity: 99.1%.

*Isobutyl(4-((4-fluorobenzyl) (prop-2-yn-1-yl)amino)phenyl)carbamate (**L1-3**).* Following procedures similar to that described for compound **L1-1** gave compound **L1-3** as yellow oil (88% over two steps). ^{1}H NMR (300 MHz, $CDCl_3$): δ 7.23−7.29 (m, 4H), 6.99 (t, J = 8.7 Hz, 2H), 6.83 (d, J = 9.3 Hz, 2H), 6.67 (s, 1H), 4.42 (s, 2H), 3.93 (s, 2H), 3.91 (d, J = 4.2 Hz, 2H), 2.21 (s, 1H), 1.92−1.97 (m, 1H), 0.94 (d, J = 6.6 Hz, 6H); ^{13}C NMR (75 MHz, $CDCl_3$): δ 163.77, 160.53, 145.32, 134.04, 129.20, 129.09, 120.72, 115.86, 115.64, 115.36, 79.54, 72.67, 71.30, 54.82, 40.42, 28.10, 19.20; HRMS (TOF ESI) m/z: calcd for $C_{21}H_{24}FN_2O_2$ $[M + H]^+$, 355.1822; found, 355.1817; HPLC purity: 99.2%.

*Allyl(4-((4-fluorobenzyl) (prop-2-yn-1-yl)amino)phenyl)carbamate (**L1-5**).* Following procedures similar to that described for compound **L1-1** gave compound **L1-5** as yellow oil (68% over two steps). ^{1}H NMR (300 MHz, $CDCl_3$): δ 7.24−7.33 (m, 4H), 7.00 (t, J = 8.4 Hz, 2H), 6.85 (d, J = 9.0 Hz, 2H), 6.65 (s, 1H), 5.88−5.99 (m, 1H), 5.33 (d, J = 17.1 Hz, 1H), 5.22 (d, J = 10.2 Hz, 1H), 4.63 (d, J = 5.7 Hz, 2H), 4.43 (s, 2H), 3.92 (s, 2H), 2.21 (s, 1H); ^{13}C NMR (75 MHz, $CDCl_3$): δ 163.82, 160.58, 145.50, 134.08, 132.79, 129.21, 118.16, 115.85, 115.69, 115.41, 79.54, 72.69, 65.85, 54.85, 40.46; HRMS (TOF ESI) m/z: calcd for $C_{20}H_{20}FN_2O_2$ $[M + H]^+$, 339.1509; found, 339.1504; HPLC purity: 95.2%.

*(2,2-Dimethyl-1,3-dioxolan-4-yl)methyl(4-((4-fluorobenzyl) (prop-2-yn-1-yl)amino)phenyl)carbamate (**L1-6**).* Following procedures similar to that described for compound **L1-1** gave compound **L1-6** as yellow oil (82% over two steps). ^{1}H NMR (300 MHz, $CDCl_3$): δ 7.23−7.29 (m, 4H), 7.00 (t, J = 8.4 Hz, 2H), 6.84 (d, J = 8.4 Hz, 2H), 4.43 (s, 2H), 4.29−4.36 (m, 1H), 4.25 (dd, J = 4.2, 0.9 Hz, 1H), 4.12 (d, J = 8.1 Hz, 1H), 4.07 (d, J = 6.9 Hz, 1H), 3.93 (s, 2H), 3.75 (dd, J = 7.2, 0.9 Hz, 1H), 2.23 (s, 1H), 1.44 (s, 3H), 1.37 (s, 3H); ^{13}C NMR (75 MHz, $CDCl_3$): δ 160.08, 156.41, 145.06, 133.58, 128.70, 120.40, 115.29, 115.22, 114.93, 109.54, 79.05, 73.58, 72.25, 65.80, 65.14, 54.36, 39.96, 26.40, 25.00; HRMS (ESI) m/z: calcd for $C_{23}H_{26}FN_2O_4$ $[M + H]^+$, 413.1877; found, 413.1869; HPLC purity: 95.0%.

*Benzyl(4-((4-fluorobenzyl) (prop-2-yn-1-yl)amino)phenyl)carbamate (**L1-7**).* Following procedures similar to that described for compound **L1-1** gave compound **L1-7** as yellow oil (60% over two steps). ^{1}H NMR (300 MHz, $CDCl_3$): δ 7.35−7.39 (m, 4H), 7.25−7.30 (m, 5H), 7.03 (d, J = 8.7 Hz, 2H), 6.85 (d, J = 8.7 Hz, 2H), 5.18 (s, 2H), 4.44 (s, 2H), 3.94 (s, 2H), 2.22 (s, 1H); ^{13}C NMR (75 MHz, $CDCl_3$): δ 163.34, 160.91, 145.38, 136.40, 134.03, 134.00, 129.15, 129.07, 128.63, 128.30, 128.28, 120.76, 115.79, 115.58, 115.37, 79.53, 72.67, 66.88, 54.77, 40.38; HRMS (TOF ESI) m/z: calcd for $C_{24}H_{22}FN_2O_4$ $[M + H]^+$, 389.1665; found, 389.1663; HPLC purity: 99.7%.

*N-(4-((4-Fluorobenzyl)(prop-2-yn-1-yl)amino)phenyl)acetamide (**L1-8**).* Following procedures similar to that described for compound

https://doi.org/10.1021/acs.jmedchem.0c02252
J. Med. Chem. 2021, 64, 5816−5837

L1-1 gave compound **L1-8** as yellow oil (20% over two steps). ^{1}H NMR (300 MHz, $CDCl_3$): δ 7.26 (d, J = 6.9 Hz, 2H), 7.05 (d, J = 8.4 Hz, 2H), 6.99 (d, J = 9.0 Hz, 2H), 6.90 (d, J = 9.0 Hz, 2H), 4.55 (s, 2H), 4.04 (s, 2H), 2.30 (s, 3H), 2.26 (t, J = 2.1 Hz, 1H); ^{13}C NMR (75 MHz, $CDCl_3$): δ 163.13, 163.18, 148.65, 133.49, 133.47, 129.65, 128.61, 115.68, 115.51, 114.61, 79.07, 72.56, 54.55, 39.87, 26.94; HRMS (TOF ESI) m/z: calcd for $C_{18}H_{18}FN_2O_4$ $[M + H]^+$, 297.1403; found, 297.1398; HPLC purity: 99.4%.

*Methyl (4-(Prop-2-yn-1-ylamino)phenyl)carbamate (**4**).* Following general procedure B, methyl (4-aminophenyl)carbamate (6.64 g, 40.0 mmol) was reacted with propargyl bromide (3.13 mL, 40.0 mmol) and DIPEA (10.48 mL, 60.0 mmol) in DMF (150 mL) at 65 °C for 4 h. Purification by flash chromatography (PE/EA, 6/1, 4/1, v/v) gave the title compound as yellow oil (4.60 g, 56%). ^{1}H NMR (300 MHz, $CDCl_3$): δ 7.20 (d, J = 7.2 Hz, 2H), 6.69 (d, J = 7.2 Hz, 2H), 6.58 (br s, 1H), 3.89 (d, J = 2.1 Hz, 2H), 3.74 (s, 3H), 2.21 (t, J = 2.1 Hz, 1H); MS (ESI) m/z: 227.1 $[M + Na]^+$.

*Methyl (4-((2-Fluorobenzyl) (prop-2-yn-1-yl)amino)phenyl)-carbamate (**L2-1**).* Following general procedure B, compound **4** (102 mg, 0.5 mmol) was reacted with 2-fluorobenzyl bromide (74 μL, 0.6 mmol) and DIPEA (0.17 mL, 1.0 mmol) in DMF (3 mL) at 65 °C for 4 h. Purification by flash chromatography (PE/EA, 15/1, 10/1, v/v) gave the title compound as yellow oil (150 mg, 96%). ^{1}H NMR (300 MHz, $CDCl_3$): δ 7.22−7.34 (m, 4H), 7.04−7.11 (m, 2H), 6.84−6.88 (m, 2H), 6.60 (br s, 1H), 4.56 (s, 2H), 4.01 (d, J = 2.4 Hz, 2H), 3.75 (s, 3H), 2.25 (t, J = 2.4 Hz, 1H); ^{13}C NMR (101 MHz, $CDCl_3$): δ 161.91, 159.96, 154.48, 145.19, 129.27, 128.82, 125.27, 124.14, 120.75, 115.42, 115.25, 79.46, 72.47, 52.23, 49.42, 40.52; HRMS (TOF ESI) m/z: calcd for $C_{18}H_{17}FN_2NaO_2$ $[M + Na]^+$: 335.1172; found, 335.1166; HPLC purity: 97.0%.

*Methyl (4-((3-Fluorobenzyl) (prop-2-yn-1-yl)amino)phenyl)-carbamate (**L2-2**).* Following procedures similar to that described for compound **L2-1** gave compound **L2-2** as yellow oil (88%). ^{1}H NMR (300 MHz, $CDCl_3$): δ 7.23−7.32 (m, 3H), 7.10 (d, J = 8.7 Hz, 1H), 7.04 (d, J = 9.0 Hz, 1H), 6.97 (td, J = 8.7, 1.8 Hz, 1H), 6.85 (d, J = 9.0 Hz, 2H), 6.57 (s, 1H), 4.48 (s, 2H), 3.98 (d, J = 2.1 Hz, 2H), 3.81 (s, 3H), 2.24 (t, J = 2.4 Hz, 1H); ^{13}C NMR (125 MHz, $CDCl_3$): δ 164.18, 162.22, 145.25, 141.33, 130.13, 122.81, 120.71, 115.48, 114.22, 114.05, 79.32, 72.55, 55.09, 52.24, 40.58; HRMS (TOF ESI) m/z: calcd for $C_{18}H_{17}FN_2NaO_2$ $[M + Na]^+$: 335.1172; found, 335.1168; HPLC purity: 97.5%.

*Methyl (4-((4-Fluoro-3-(trifluoromethyl)benzyl) (prop-2-yn-1-yl)-amino)phenyl)carbamate (**L2-3**).* Following procedures similar to that described for compound **L2-1** gave compound **L2-3** as yellow oil (87%). ^{1}H NMR (300 MHz, $CDCl_3$): δ 7.50−7.59 (m, 2H), 7.25 (d, J = 8.7 Hz, 2H), 7.15 (t, J = 9.0 Hz, 1H), 6.86 (d, J = 8.7 Hz, 2H), 6.49 (br s, 1H), 4.48 (s, 2H), 3.96 (d, J = 2.4 Hz, 2H), 3.69 (s, 3H), 2.27 (t, J = 2.4 Hz, 1H); ^{13}C NMR (125 MHz, $CDCl_3$): δ 159.95, 157.92, 145.00, 134.72, 132.71, 126.01, 123.66, 121.49, 120.67, 117.14, 1159.9, 78.99, 72.91, 54.63, 52.26, 40.81; HRMS (TOF ESI) m/z: calcd for $C_{19}H_{16}F_4N_2NaO_2$ $[M + Na]^+$: 403.1046; found, 403.1042; HPLC purity: 97.4%.

*Methyl (4-((3,4-Difluorobenzyl) (prop-2-yn-1-yl)amino)phenyl)-carbamate (**L2-4**).* Following procedures similar to that described for compound **L2-1** gave compound **L2-4** as yellow oil (15%). ^{1}H NMR (300 MHz, $CDCl_3$): δ 7.26 (d, J = 8.7 Hz, 2H), 7.05−7.18 (m, 3H), 6.85 (d, J = 8.7 Hz, 2H), 6.47 (br s, 1H), 4.42 (s, 2H), 3.96 (d, J = 2.1 Hz, 2H), 3.75 (s, 3H), 2.23 (t, J = 2.4 Hz, 1H); ^{13}C NMR (125 MHz, $CDCl_3$): δ 151.59, 149.51, 148.6, 145.10, 135.57, 123.17, 120.68, 117.32, 116.30, 115.80, 79.17, 72.74, 54.66, 52.27, 40.69; HRMS (TOF ESI) m/z: calcd for $C_{18}H_{16}F_2N_2NaO_2$ $[M + Na]^+$: 353.1073; found, 353.1073; HPLC purity: 97.0%.

*Methyl (4-((2-Chlorobenzyl) (prop-2-yn-1-yl)amino)phenyl)-carbamate (**L2-5**).* Following procedures similar to that described for compound **L2-1** gave compound **L2-5** as yellow oil (81%). ^{1}H NMR (300 MHz, $CDCl_3$): δ 7.30−7.41 (m, 2H), 7.19−7.25 (m, 4H), 6.85 (d, J = 8.7 Hz, 2H), 6.46 (br s, 1H), 4.59 (s, 2H), 4.06 (d, J = 2.4 Hz, 2H), 3.75 (s, 3H), 2.25 (t, J = 2.4 Hz, 1H); ^{13}C NMR (125 MHz, $CDCl_3$): δ 154.52, 144.94, 135.52, 133.06, 129.58, 128.44, 126.92, 120.89, 114.54, 79.54, 72.45, 53.63, 52.23, 40.73; HRMS (TOF ESI) m/z: calcd for $C_{18}H_{18}ClN_2O_2$ $[M + H]^+$, 329.1057; found, 329.0873; HPLC purity: 99.4%.

*Methyl (4-((3-Methoxybenzyl) (prop-2-yn-1-yl)amino)phenyl)-carbamate (**L2-6**).* Following procedures similar to that described for compound **L2-1** gave compound **L2-6** as yellow oil (27%). ^{1}H NMR (300 MHz, $CDCl_3$): δ 7.22−7.26 (m, 4H), 6.85−6.90 (m, 4H), 6.43 (br s, 1H), 4.42 (s, 2H), 3.93 (d, J = 2.1 Hz, 2H), 3.80 (s, 3H), 3.78 (s, 3H), 2.20 (t, J = 2.4 Hz, 1H); ^{13}C NMR (125 MHz, $CDCl_3$): δ 159.96, 145.51, 140.16, 129.63, 120.73, 119.61, 115.33, 112.84, 112.62, 79.61, 72.35, 55.42, 55.20, 52.22, 40.35; HRMS (TOF ESI) m/z: calcd for $C_{19}H_{20}N_2NaO_3$ $[M + Na]^+$: 347.1372; found, 347.1373; HPLC purity: 97.5%.

*Methyl (4-((4-Bromobenzyl) (prop-2-yn-1-yl)amino)phenyl)-carbamate (**L2-7**).* Following procedures similar to that described for compound **L2-1** gave compound **L2-7** as yellow oil (15%). ^{1}H NMR (300 MHz, $CDCl_3$): δ 7.45 (d, J = 8.1 Hz, 2H), 7.25 (d, J = 8.4 Hz, 2H), 7.19 (d, J = 8.4 Hz, 2H), 6.84 (d, J = 8.4 Hz, 2H), 6.71 (s, 1H), 4.43 (s, 2H), 3.95 (d, J = 2.1 Hz, 2H), 3.75 (s, 3H), 2.24 (t, J = 2.1 Hz, 1H); ^{13}C NMR (125 MHz, $CDCl_3$): δ 154.47, 137.41, 131.68, 129.11, 128.57, 121.40, 120.97, 115.64, 79.28, 72.57, 54.91, 52.25, 40.53; HRMS (TOF ESI) m/z: calcd for $C_{18}H_{18}BrN_2O_2$ $[M + H]^+$, 373.0552; found, 373.0352; HPLC purity: 98.2%.

*Methyl (4-((4-Methylbenzyl) (prop-2-yn-1-yl)amino)phenyl)-carbamate (**L2-8**).* Following procedures similar to that described for compound **L2-1** gave compound **L2-8** as yellow oil (81%). ^{1}H NMR (300 MHz, $CDCl_3$): δ 7.15−7.23 (m, 4H), 6.99 (t, J = 8.7 Hz, 2H), 6.63 (d, J = 9.0 Hz, 2H), 6.53 (s, 1H), 4.44 (s, 2H), 4.18 (t, J = 2.1 Hz, 2H), 3.74 (s, 3H), 2.34 (s, 3H), 2.25 (t, J = 2.1 Hz, 1H); ^{13}C NMR (125 MHz, $CDCl_3$): δ 145.65, 136.82, 135.18, 129.27, 127.37, 120.72, 115.43, 79.60, 72.23, 55.07, 52.23, 40.13, 21.08; HRMS (TOF ESI) m/z: calcd for $C_{19}H_{21}N_2O_2$ $[M + H]^+$, 309.1603; found, 309.1546; HPLC purity: 99.9%.

*Methyl (2-Aminophenyl)carbamate (**6a**).* To a solution of *o*-phenylenediamine **5a** (1.08 g, 10.0 mmol) in DCM (50 mL) was added DIPEA (3.49 mL, 20.0 mmol). At −20 °C, a solution of methyl chloroformate (0.78 mL, 10.0 mmol) DCM (10 mL) was added dropwise via a syringe. The reaction mixture was allowed to warm to room temperature and stirred for further 2 h. After completion, the mixture was washed with water, brine, dried over anhydrous Na_2SO_4, and filtered. The filtrate was concentrated to dryness in vacuo. Purification by flash chromatography (PE/EA, 4/1, 2/1, v/v) gave title compound **6a** as a yellow solid (1.14 g, 69%). ^{1}H NMR (300 MHz, $CDCl_3$): δ 7.24−7.27 (m, 1H), 7.03 (t, J = 7.2 Hz, 1H), 6.76−6.81 (m, 2H), 6.41 (br s, 1H), 3.77 (s, 3H); MS (ESI) m/z: 189.1 $[M + Na]^+$.

*Methyl (2-(Prop-2-yn-1-ylamino)phenyl)carbamate (**7a**).* Following general procedure B, compound **6a** (0.67 g, 4.0 mmol) was reacted with propargyl bromide (313 μL, 4.0 mmol) and DIPEA (1.05 mL, 6.0 mmol) in DMF (20 mL) at 65 °C for 4 h. After completion, purification by flash chromatography (PE/EA, 4/1, 2/1, v/v) gave the title compound **7a** as yellow oil (0.74 g, 90%). ^{1}H NMR (300 MHz, $CDCl_3$): δ 7.34 (d, J = 8.1 Hz, 1H), 7.16 (td, J = 8.4, 1.5 Hz, 1H), 6.83−6.88 (m, 2H), 6.32 (br s, 1H), 3.92 (d, J = 2.1 Hz, 2H), 3.77 (s, 2H), 2.24 (t, J = 2.1 Hz, 1H); MS (ESI) m/z: 227.0 $[M + Na]^+$.

*Methyl (2-((4-Fluorobenzyl) (prop-2-yn-1-yl)amino)phenyl)-carbamate (**L3-1**).* Following general procedure B, compound **7a** (0.102 g, 0.5 mmol) was reacted with *p*-fluorobenzyl bromide (74 μL, 0.55 mmol) and DIPEA (174 μL, 1.0 mmol) in DMF (3 mL) at 65 °C for 4 h. After completion, purification by flash chromatography (PE/EA, 15/1, 10/1, v/v) gave title compound **L3-1** as yellow oil (150 mg, 96%). ^{1}H NMR (300 MHz, $CDCl_3$): δ 8.10 (d, J = 8.4 Hz, 1H), 7.86 (s, 1H), 7.35 (dd, J = 8.4, 1.2 Hz, 1H), 7.28 (ddd, J = 8.1, 4.8, 3.0 Hz, 2H), 7.18 (dd, J = 7.8, 1.2 Hz, 1H), 7.00 (ddd, J = 9.0, 4.8, 2.7 Hz, 2H), 4.11 (s, 2H), 3.79 (s, 3H), 3.56 (d, J = 2.4 Hz, 2H), 2.27 (t, J = 2.4 Hz, 1H); ^{13}C NMR (125 MHz, $CDCl_3$): δ 164.14, 160.89, 156.30, 154.15, 138.32, 134.48, 133.03, 131.03, 126.69, 123.79, 122.72, 118.11, 115.52, 78.89, 74.19, 56.40, 52.48, 42.69; HRMS (TOF ESI) m/z: calcd for $C_{18}H_{18}FN_2O_2$ $[M + H]^+$, 313.1352; found, 313.1354; HPLC purity: 95.3%.

https://doi.org/10.1021/acs.jmedchem.0c02252
J. Med. Chem. 2021, 64, 5816−5837

*Methyl (3-Aminophenyl)carbamate (**6b**).* Following procedures similar to that described for **6a**, using benzene-1,3-diamine **5b** (1.08 g, 10.0 mmol), gave the title compound **6b** as a yellow solid (1.0 g, 60%). ^{1}H NMR (300 MHz, $CDCl_3$): δ 7.05 (t, J = 8.4 Hz, 1H), 6.94 (s, 1H), 6.59 (d, J = 8.4 Hz, 1H), 6.53 (s, 1H), 6.38 (d, J = 8.4 Hz, 1H), 3.76 (s, 3H); MS (ESI) m/z: 167.1 $[M + H]^+$.

*Methyl (3-(Prop-2-yn-1-ylamino)phenyl)carbamate (**7b**).* Following procedures similar to that described for **7a**, using compound **6b** (0.67 g, 4.0 mmol), gave the title compound **7b** as yellow oil (205 mg, 25%). ^{1}H NMR (300 MHz, $CDCl_3$): δ 7.11 (t, J = 8.1 Hz, 1H), 6.89 (s, 1H), 6.67 (d, J = 8.1 Hz, 1H), 6.40 (d, J = 8.1 Hz, 1H), 3.99 (s, 2H), 3.75 (s, 3H), 2.21 (s, 1H); MS (ESI) m/z: 227.0 $(M + Na^+)$.

*Methyl (3-((4-Fluorobenzyl) (prop-2-yn-1-yl)amino)phenyl)-carbamate (**L3-2**).* Following procedures similar to that described for compound **L3-1**, using compound **7b** (0.102 g, 0.5 mmol), gave the title compound **L3-2** as yellow oil (128 mg, 82%). ^{1}H NMR (300 MHz, $CDCl_3$): δ 7.28 (t, J = 8.1 Hz, 2H), 7.19 (t, J = 8.7 Hz, 2H), 6.95−7.07 (m, 3H), 6.77 (d, J = 8.7 Hz, 1H), 6.56−6.62 (m, 2H), 4.51 (s, 2H), 3.99 (d, J = 2.4 Hz, 2H), 3.75 (s, 3H), 2.23 (t, J = 2.4 Hz, 1H); ^{13}C NMR (125 MHz, $CDCl_3$): δ 163.97, 160.72, 147.94, 146.00, 144.82, 134.00, 129.49, 115.00, 110.08, 109.99, 79.38, 72.85, 54.97, 51.71, 40.80; HRMS (TOF ESI) m/z: calcd for $C_{18}H_{18}FN_2O_2$ $[M + H]^+$, 313.1352; found, 313.1344; HPLC purity: 98.0%.

*Methyl (2-Fluoro-5-nitrophenyl)carbamate (**6c**).* Under a nitrogen atmosphere, sodium hydride (60% dispersion in mineral oil, 200 mg, 5.0 mmol) was added in portions to a solution of 2-fluoro-5-nitroaniline **5c** (785 mg, 5.0 mmol) in dry THF (25 mL) at 0 °C. After the reaction mixture was stirred for 30 min, it was allowed to warm to room temperature and stirred for further 1 h. A solution of methyl chloroformate (0.39 mL, 5.0 mmol) in dry THF (25 mL) was added dropwise via a syringe, and the resulting mixture was stirred for further 30 min. After completion, the reaction was quenched with water and extracted with EA. The combined organic phase was washed with brine, dried over anhydrous Na_2SO_4, filtered, and concentrated to dryness in vacuo. Purification by flash chromatography (PE/EA, 4/1, v/v) gave title compound **6c** as a yellow solid (428 mg, 40%). ^{1}H NMR (300 MHz, $CDCl_3$): δ 9.08 (d, J = 6.9 Hz, 1H), 7.94 (t, J = 9.0 Hz, 1H), 7.21 (d, J = 9.0 Hz, 1H), 7.01 (s, 1H), 3.87 (s, 3H); MS (ESI) m/z: 237.0 $[M + Na]^+$.

*Methyl (5-Amino-2-fluorophenyl)carbamate (**6d**).* Following method A of general procedure F, catalytic hydrogenation of compound **6c** (428 mg, 2.0 mmol) gave compound **6d** quantitatively and was used without purification. ^{1}H NMR (300 MHz, $CDCl_3$): δ 7.49 (s, 1H), 6.81−-6.86 (m, 2H), 6.26−-6.28 (d, J = 6Hz, 1H), 3.87 (s, 3H), 3.59 (br s, 2H); MS (ESI) m/z: 207.0 $[M + Na]^+$.

*Methyl (2-Fluoro-5-((4-fluorobenzyl) (prop-2-yn-1-yl)amino)-phenyl)carbamate (**L3-3**).* Following procedures similar to that described for **7a**, using compound **6d** (368 mg, 2 mmol), gave intermediate **7c** as yellow oil (187 mg, 42%). MS (ESI) m/z: 245.0 $[M + Na]^+$; further following a procedure similar to that described for compound **L3-1**, using compound **7c** (90 mg, 0.41 mmol), gave final compound **L3-3** as yellow oil (112 mg, 83%). ^{1}H NMR (300 MHz, $CDCl_3$): δ 7.79 (br s, 1H), 7.29 (ddd, J = 9.0, 5.4, 2.4 Hz, 2H), 7.02 (ddd, J = 8.7, 5.1, 2.7 Hz, 2H), 6.93 (dd, J = 10.2, 9.0 Hz, 1H), 6.83 (br s, 1H), 6.50 (ddd, J = 9.0, 5.4, 3.3 Hz, 1H), 4.44 (s, 2H), 3.95 (d, J = 2.1 Hz, 2H), 3.79 (s, 3H), 2.41 (t, J = 2.1 Hz, 1H); ^{13}C NMR (125 MHz, $CDCl_3$): δ 163.08, 161.13, 153.65, 145.75, 133.72, 129.22, 115.48, 114.96, 109.83, 107.31, 79.12, 72.59, 54.74, 52.47, 40.57; HRMS (TOF ESI) m/z: calcd for $C_{18}H_{17}F_2N_2O_2$ $[M + H]^+$, 331.1258; found, 331.1251; HPLC purity: 96.0%.

*tert-Butyl (2-Fluoro-4-nitrophenyl)carbamate (**8**).* Following general procedure E, 2-fluoro-4-nitroaniline **5d** (624 mg, 4.0 mmol) was reacted with Boc_2O (963 mg, 4.4 mmol), TEA (837 μL, 4.8 mmol), and DMAP (49 mg, 0.4 mmol) in DCM (20 mL) at room temperature overnight. Purification by flash chromatography (PE/EA, 25/1, v/v) gave compound **8** as a yellow solid (747 mg, 73%). ^{1}H NMR (300 MHz, $CDCl_3$): δ 7.99−8.07 (m, 2H), 7.38 (t, J = 7.2 Hz, 1H), 1.43 (s, 9H); MS (ESI) m/z: 257.1 $[M + H]^+$.

*Methyl (2-Fluoro-4-((4-fluorobenzyl) (prop-2-yn-1-yl)amino)-phenyl)carbamate (**L3-4**).* Following the procedure similar to that described for compound **6c**, using compound **8** (512 mg, 2.0 mmol), gave intermediate **9** after flash chromatography (PE/EA, 10/1, v/v) as yellow oil (362 mg, 58%); the above-obtained oil (362 mg, 1.15 mmol) was reduced following method A of general procedure F to give the respective amine quantitatively; following general procedure B, the obtained amine was reacted with propargyl bromide (90 μL, 1.15 mmol) and DIPEA (0.38 mL, 2.2 mmol) in DMF (10 mL) at 65 °C for 4 h. Purification by flash chromatography (PE/EA, 5/1, 4/1, v/v) gave yellow oil (162 mg, 44%); further following general procedure B, the above-obtained oil (120 mg, 0.37 mmol) was reacted with *p*-fluorobenzyl bromide (50 μL, 0.37 mmol) and DIPEA (64 μL, 0.37 mmol) in DMF (5 mL) at 65 °C for 4 h. Purification by flash chromatography (PE/EA, 15/1, 10/1, v/v) gave yellow oil (132 mg, 83%); following general procedure C, the above-obtained oil (120 mg, 0.28 mmol) was deprotected using TFA (0.2 mL) in DCM (2 mL) and gave compound **L3-4** as yellow oil after purification by flash chromatography (PE/EA, 8/1, 6/1, v/v) (76 mg, 83%). ^{1}H NMR (300 MHz, $CDCl_3$): δ 7.78 (br s, 1H), 7.24−7.29 (m, 2H), 7.02 (t, J = 8.7 Hz, 2H), 6.60−6.66 (m, 2H), 6.51 (br s, 1H), 4.45 (s, 2H), 3.96 (d, J = 2.1 Hz, 2H), 3.77 (s, 3H), 2.24 (t, J = 2.1 Hz, 1H); ^{13}C NMR (125 MHz, $CDCl_3$): δ 163.36, 160.93, 133.46, 128.89, 115.65, 115.44, 110.45, 102.08, 101.85, 78.99, 72.76, 54.61, 52.45, 40.27; HRMS (TOF ESI) m/z: calcd for $C_{18}H_{16}F_2N_2NaO_2$ $[M + Na]^+$: 353.1078; found, 353.1068; HPLC purity: 97.1%.

*2-Fluoro-N-(4-fluorobenzyl)-4-nitroaniline (**10**).* Following general procedure A, 2-fluoro-4-nitroaniline **5d** (624 mg, 4.0 mmol) was condensed with *p*-fluorobenzaldehyde (0.43 mL, 4.0 mmol) catalyzed by *p*-TsOH (17 mg, 0.1 mmol) in toluene (20 mL) after reflux for 3 h, followed by reduction by $NaBH_4$ (380 mg, 10.0 mmol) in MeOH (20 mL) at room temperature for 2 h. Purification by flash chromatography (PE/EA, 8/1, 6/1, v/v) gave the title compound **10** as a light yellow solid (982 mg, 93% over two steps). ^{1}H NMR (300 MHz, $CDCl_3$): δ 7.98−7.90 (m, 3H), 7.33−7.31 (m, 2H), 7.08−7.06 (m, 2H), 6.61 (br s, 1H), 5.03 (s, 1H), 4.45 (s, 2H); MS (ESI) m/z: 287.0 $[M + Na]^+$.

*Methyl (3-Fluoro-4-((4-fluorobenzyl) (prop-2-yn-1-yl)amino)-phenyl)carbamate (**L3-5**).* To a solution of compound **10** (264 mg, 1.0 mmol) in dry DMF (5 mL) was added sodium hydride (60% dispersed in mineral oil, 44 mg, 1.1 mmol) in portions at 0 °C under a nitrogen atmosphere. After the mixture was stirred for 30 min, propargyl bromide (94 μL, 1.2 mmol) was added and the reaction mixture was stirred at 65 °C for further 4 h. After completion, the reaction was quenched with water and extracted with EA. The combined organic phase was washed with brine, dried over anhydrous Na_2SO_4, filtered, and concentrated to dryness in vacuo. The purification of the residue by flash chromatography (PE/EA, 10/1, v/v) gave a yellow solid (260 mg, 86%).

The above-obtained yellow solid (260 mg, 0.86 mmol) was reduced to the respective amine following method B of general procedure F, using the Fe powder (200 mg) in EtOH/AcOH (20 mL/0.5 mL) after reflux for 3 h. Purification by flash chromatography (PE/EA, 6/1, v/v) afforded the desired product as a yellow solid (166 mg, 71%). ^{1}H NMR (300 MHz, $CDCl_3$): δ 7.35−7.37 (m, 2H), 6.98−7.00 (m, 3H), 6.35−6.44 (m, 2H), 4.18 (s, 2H), 3.68 (br s, 2H), 2.25 (s, 1H); MS (ESI) m/z: 273.1 $[M + H]^+$.

Following general procedure D, the above-obtained amine intermediate (100 mg, 0.37 mmol) was reacted with methyl chloroformate (34 μL, 0.44 mmol) and DIPEA (96 μL, 0.56 mmol) in DCM (5 mL) at room temperature for 1 h. After completion, the crude product was purified by flash chromatography (PE/EA, 10/1, v/v) to give the final compound **L3-5** as yellow oil (98 mg, 81%). ^{1}H NMR (300 MHz, $CDCl_3$): δ 7.78 (br s, 1H), 7.24−7.29 (m, 2H), 7.02 (t, J = 8.7 Hz, 2H), 6.60−6.66 (m, 2H), 6.51 (br s, 1H), 4.45 (s, 2H), 3.96 (d, J = 2.1 Hz, 2H), 3.77 (s, 3H), 2.24 (t, J = 2.1 Hz, 1H); ^{13}C NMR (125 MHz, $CDCl_3$): δ 162.17, 161.22, 157.09, 155.13, 153.95, 133.31, 130.34, 122.11, 115.31, 114.19, 78.94, 73.49, 54.71, 52.42, 40.80; HRMS (TOF ESI) m/z: calcd for $C_{18}H_{17}F_2N_2O_2$ $[M + H]^+$, 331.1258; found, 331.1251; HPLC purity: 97.6%.

*tert-Butyl (4-Amino-2-chlorophenyl)carbamate (**11**).* Following general procedure E, 2-chloro-4-nitroaniline **5e** (692 mg, 4.0 mmol)

https://doi.org/10.1021/acs.jmedchem.0c02252
J. Med. Chem. 2021, 64, 5816−5837

was reacted with Boc_2O (963 mg, 4.4 mmol) in the presence of TEA (0.84 mL, 6.0 mmol) and DMAP (49 mg, 0.4 mmol) in DCM (20 mL), gave its N-Boc-protected product as a yellow solid after purification by flash chromatography (PE/EA, 25/1, v/v) (400 mg, 37%).

Following method A of general procedure F, catalytic hydrogenation of the above-obtained solid (400 mg, 1.47 mmol) gave amine **11** quantitatively and was used without purification. ^{1}H NMR (300 MHz, $CDCl_3$): δ 7.24−7.28 (s, 1H), 7.07−7.10 (d, J = 9.0 Hz, 1H), 6.80−6.83 (d, J = 9.0 Hz 1H), 4.12 (br s, 2H), 1.43 (s, 9H); MS (ESI) m/z: 243.0 $[M + H]^+$.

*tert-Butyl (2-Chloro-4-((4-fluorobenzyl)amino)phenyl)-carbamate (**12**).* Following general procedure B, compound **11** (360 mg, 1.48 mmol) was reacted with *p*-fluorobenzyl bromide (0.2 mL, 1.48 mmol) in the presence of DIPEA (0.52 mL, 2.96 mmol) in DMF (5 mL) at 65 °C for 4 h. Purification by flash chromatography (PE/EA, 10/1, 6/1, v/v) gave intermediate **12** as yellow oil (430 mg, 83%). ^{1}H NMR (300 MHz, $CDCl_3$): δ 7.24−7.28 (m, 2H), 6.98−7.06 (m, 3H), 6.55−6.62 (m, 2H), 4.53 (s, 2H), 1.43 (s, 9H); MS (ESI) m/z: 351.1 $[M + H]^+$.

*Methyl (2-Chloro-4-((4-fluorobenzyl) (prop-2-yn-1-yl)amino)-phenyl)carbamate (**L3-6**).* Following general procedure B, intermediate **12** (35 mg, 0.1 mmol) was reacted with propargyl bromide (11.9 μL, 0.15 mmol) in the presence of DIPEA (35.0 μL, 0.2 mmol) in DMF (2 mL) at 65 °C for 4 h. Purification by flash chromatography (PE/EA, 10/1, v/v) afforded yellow oil (36.9 mg, 95%).

The above-obtained oil (36.9 mg, 0.095 mmol) was then deprotected following general procedure C in DCM (1 mL) using TFA (0.1 mL). Following general procedure C, the deprotected product was then reacted with methyl chloroformate (12 μL, 0.15 mmol) in presence of DIPEA (35 μL, 0.2 mmol) in DCM (1 mL) at room temperature for 1 h. Further purification by flash chromatography (PE/EA, 8/1, v/v) gave final compound **L3-6** as yellow oil (28 mg, 85% over two steps). ^{1}H NMR (300 MHz, $CDCl_3$): δ 7.88 (d, J = 8.7 Hz, 1H), 7.24−7.29 (m, 2H), 6.98−7.06 (m, 2H), 6.89 (d, J = 2.7 Hz, 1H), 6.81 (dd, J = 9.0, 3.0 Hz, 2H), 4.44 (s, 2H), 3.94 (d, J = 2.1 Hz, 2H), 3.78 (s, 3H), 2.24 (t, J = 2.1 Hz, 1H); ^{13}C NMR (125 MHz, $CDCl_3$): δ 163.13, 161.18, 154.11, 145.55, 133.36, 128.95, 126.30, 115.62, 114.39, 78.85, 72.80, 54.55, 52.44, 40.21; HRMS (TOF ESI) m/z: calcd for $C_{18}H_{17}ClFN_2O_2$ $[M + H]^+$, 347.0963; found, 347.0779; HPLC purity: 99.3%.

*tert-Butyl Methyl (2-Chloro-1,4-phenylene)dicarbamate (**13**).* Following general procedure C, compound **11** (242 mg, 1.0 mmol) was reacted with methyl chloroformate (117 μL, 1.5 mmol) in the presence of DIPEA (350 μL, 2.0 mmol) in DCM (10 mL). Purification by flash chromatography (PE/EA, 8/1) gave compound **13** as yellow oil (285 mg, 95%). ^{1}H NMR (300 MHz, $CDCl_3$): δ 7.59 (s, 1H), 7.23−7.26 (d, J = 9.0 Hz, 1H), 7.09−7.12 (d, J = 9.0 Hz 1H), 6.92 (br s, 1H), 3.78 (s, 3H), 1.43 (s, 9H); MS (ESI) m/z: 301.1 $[M + H]^+$.

*Methyl (3-Chloro-4-((4-fluorobenzyl) (prop-2-yn-1-yl)amino)-phenyl)carbamate (**L3-7**).* The above-obtained compound **13** (285 mg, 0.95 mmol) was deprotected following general procedure C in DCM (3 mL) and TFA (0.3 mL) at room temperature for 2 h. Purification by flash chromatography (PE/EA, 4/1) gave the respective amine intermediate as a pale yellow solid (148 mg, 78%).

Following general procedure B, the above-obtained amine intermediate (148 mg, 0.74 mmol) was then reacted with *p*-fluorobenzyl bromide (100 μL, 0.74 mmol) in the presence of DIPEA (0.26 mL, 1.48 mmol) in DMF (5 mL) at 65 °C for 4 h. Purification by flash chromatography (PE/EA, 8/1, 6/1, v/v) gave a yellow solid (143 mg, 63%).

Following general procedure B, the above-obtained solid (62 mg, 0.2 mmol) was further reacted with propargyl bromide (24 μL, 0.3 mmol) in the presence of DIPEA (70 μL, 0.4 mmol) in DMF (2 mL) at 65 °C for 4 h. Purification by flash chromatography (PE/EA, 8/1, v/v) gave final compound **L3-7** as yellow oil (66 mg, 95%). ^{1}H NMR (300 MHz, $CDCl_3$): δ 7.51 (d, J = 2.4 Hz, 1H), 7.39−7.43 (m, 2H), 7.24 (d, J = 8.7 Hz, 1H), 7.18 (dd, J = 8.7, 2.4 Hz, 1H), 6.97−7.04 (m, 2H), 6.52 (s, 1H), 4.23 (s, 2H), 3.77 (s, 3H), 3.73 (d, J = 2.1 Hz, 2H), 2.26 (t, J = 2.1 Hz, 1H); ^{13}C NMR (125 MHz, $CDCl_3$): δ 163.35, 160.92, 153.90, 142.70, 133.38, 130.55, 130.28, 124.24, 115.30, 78.79, 73.61, 54.89, 52.49, 41.41; HRMS (TOF ESI) m/z: calcd for $C_{18}H_{17}ClFN_2O_2$ $[M + H]^+$, 347.0963; found, 347.0981; HPLC purity: 95.7%.

*N^1-(4-Fluorobenzyl)-3-methylbenzene-1,4-diamine (**14**).* Following general procedure B, 3-methyl-4-nitroaniline **5f** (1.52 g, 10.0 mmol) was reacted with *p*-fluorobenzyl bromide (1.35 mL, 10.0 mmol) and DIPEA (3.5 mL, 20.0 mmol) in DMF (25 mL) at 65 °C overnight. Crystallization of the crude product in EA/PE (15 mL/45 mL) gave a yellow solid (1.25 g, 48%); following method A of general procedure F, this solid was further hydrogenated to afford compound **14** quantitatively. ^{1}H NMR (300 MHz, $CDCl_3$): δ 7.30−7.32 (m, 2H), 7.03−7.05 (m, 3H), 6.77 (s, 1H), 6.74−6.75 (m, 2H), 4.47 (s, 2H), 2.24 (s, 3H); MS (ESI) m/z: 231.1 $[M + H]^+$.

*Methyl (4-((4-Fluorobenzyl) (prop-2-yn-1-yl)amino)-2-methylphenyl)carbamate (**L3-8**).* To an ice-cooled solution of the above-obtained compound **14** (1.10 g, 0.48 mmol) in THF/H_20 (40 mL/20 mL) was added $NaHCO_3$ (604 mg, 7.2 mmol) and Boc_2O (1.05 g, 4.8 mmol). 30 min later, the mixture was allowed to warm to room temperature and stirred overnight. After completion, the mixture was poured into water (50 mL) and extracted with EA. The combined organic phase was washed with brine, dried over anhydrous Na_2SO_4, filtered, and concentrated in vacuo. The residue was further purified by flash chromatography (PE/EA, 8/1, 6/1, v/v) to give an off-white solid (1.42 g, 90%).

Following general procedure B, the above-obtained solid (660 mg, 2.0 mmol) was reacted with propargyl bromide (0.24 mL, 3.0 mmol) and DIPEA (0.7 mL, 4.0 mmol) in DMF (2 mL) at 65 °C for 4 h. Flash chromatography (PE/EA, 10/1, v/v) gave a white solid (662 mg, 90%). ^{1}H NMR (300 MHz, $CDCl_3$): δ 7.30−7.32 (m, 2H), 7.03−7.05 (m, 2H), 6.77 (s, 1H), 6.74−6.75 (m, 2H), 4.47 (s, 2H), 3.96 (s, 2H), 2.24 (s, 3H), 2.23 (s, 1H) 1.53 (s, 9H); MS (ESI) m/z: 369.2 $[M + H]^+$.

Following general procedure C, the above-obtained solid (180 mg, 0.49 mmol) was deprotected using TFA (0.4 mL) in DCM (4 mL) at room temperature for 1 h; further following general procedure D, the deprotected product was further reacted with methyl chloroformate (117 μL, 1.5 mmol) in the presence of DIPEA (174 μL, 1.0 mmol) in DCM (1 mL) at room temperature for 1 h. Flash chromatography (PE/EA, 6/1, v/v) gave final compound **L3-8** as pale yellow oil (135 mg, 85%). ^{1}H NMR (300 MHz, $CDCl_3$): δ 7.41 (br s, 1H), 7.26−7.31 (m, 2H), 6.99−7.05 (m, 2H), 6.73−6.76 (m, 2H), 6.23 (s, 1H), 4.46 (s, 2H), 3.96 (d, J = 2.1 Hz, 2H), 3.76 (s, 3H), 2.22−2.24 (m, 4H); ^{13}C NMR (75 MHz, $CDCl_3$): δ 163.05, 161.10, 146.3, 133.96, 128.93, 127.14, 124.32, 116.66, 115.50, 113.18, 79.40, 72.38, 54.52, 52.35, 40.08, 18.23; HRMS (TOF ESI) m/z: calcd for $C_{19}H_{20}FN_2O_2$ $[M + H]^+$, 327.1509; found, 327.1503; HPLC purity: 99.0%.

*tert-Butyl (4-((4-Fluorobenzyl)amino)-3-methylphenyl)-carbamate (**15**).* Following general procedure E, 3-methyl-4-nitroaniline **5f** (1.52 g, 10.0 mmol) was reacted in DCM (40 mL) with Boc_2O (2.18 g, 10.0 mmol) in the presence of TEA (1.67 mL, 12.0 mmol) and DMAP (0.122 g, 1.0 mmol) to give the N-Boc-protected intermediate as a pale yellow solid after flash chromatography (PE/EA, 10/1, v/v) (1.9 g, 75%).

Following method A of general procedure F, the above-obtained solid was hydrogenated in EA (40 mL) using 10% Pd−C (75 mg) to give the respective amine in a quantitative yield.

Following general procedure A, the above-obtained amine (1.62 g, 7.3 mmol) was condensed in toluene with *p*-fluorobenzaldehyde (0.81 mL, 7.5 mmol) catalyzed by *p*-TsOH (32 mg, 0.19 mmol), followed by reduction by $NaBH_4$ (570 mg, 15.0 mmol) in MeOH (20 mL) at room temperature for 2 h, giving compound **15** as a yellow solid after flash chromatography (PE/EA, 10/1, v/v) (1.78 g, 74%). ^{1}H NMR (300 MHz, $CDCl_3$): δ 7.31−7.35 (m, 2H), 7.15 (s, 1H), 6.96−7.05 (m, 3H), 6.49 (d, J = 8.1 Hz, 1H), 6.29 (s, 1H), 4.33 (s, 2H), 2.15 (s, 3H), 1.46 (s, 9H).

*Methyl (4-((4-Fluorobenzyl) (prop-2-yn-1-yl)amino)-3-methylphenyl)carbamate (**L3-9**).* Following general procedure B,

https://doi.org/10.1021/acs.jmedchem.0c02252
J. Med. Chem. 2021, 64, 5816−5837

compound **15** (165 mg, 0.5 mmol) was reacted in DMF (2 mL) with propargyl bromide (59 μL, 0.75 mmol) in the presence of DIPEA (175 μL, 1.0 mmol) at 65 °C for 4 h, giving pale yellow oil after purification by flash chromatography (PE/EA, 8/1, v/v) (165 mg, 90%).

The above-obtained product (165 mg, 0.45 mmol) was deprotected following general procedure C, using TFA (0.2 mL) in DCM (2 mL) at room temperature for 1 h. Following general procedure D, the deprotected amine was then reacted in DCM (2 mL) with methyl chloroformate (53 μL, 0.68 mmol) and DIPEA (157 μL, 0.9 mmol) at room temperature for 1 h. Further purification by flash chromatography (PE/EA, 6/1, v/v) gave title compound **L3-9** as a pale yellow solid (122 mg, 83%). ^{1}H NMR (300 MHz, $CDCl_3$): δ 7.35 (dd, *J* = 8.4, 5.7 Hz, 2H), 7.17−7.26 (m, 3H), 6.97−7.03 (m, 2H), 6.75 (s, 1H), 4.15 (s, 2H), 3.76 (s, 3H), 3.56 (d, *J* = 2.1 Hz, 2H), 2.33 (s, 3H), 2.25 (t, *J* = 2.1 Hz, 1H); ^{13}C NMR (125 MHz, $CDCl_3$): δ 163.04, 161.10, 154.15, 145.08, 134.80, 133.98, 130.38, 123.34, 115.22, 79.14, 73.27, 55.53, 52.29, 42.09, 18.08; HRMS (TOF ESI) *m*/*z*: calcd for $C_{19}H_{20}FN_2O_2$ $[M + H]^+$, 327.1509; found, 327.1502; HPLC purity: 95.2%.

*Methyl (4-(Prop-2-yn-1-ylamino)-2-(trifluoromethyl)phenyl)-carbamate (**17**).* Following method A of general procedure F, 4-nitro-2-(trifluoromethyl)aniline **5g** (1.03 g, 5.0 mmol) was hydrogenated in EtOAc (30 mL) using 10% Pd/C (38 mg) as the catalyst to give amine product 2-(trifluoromethyl)benzene-1,4-diamine in a quantitative yield.

Following general procedure E, above-obtained 2-(trifluoromethyl)benzene-1,4-diamine was reacted in DCM (40 mL) with Boc_2O (1.10 g, 5.0 mmol) in presence of TEA (0.84 mL, 6.0 mmol), and DMAP (61 mg, 0.5 mmol) at room temperature overnight. Purification by flash chromatography (PE/EA, 10/1, v/v) gave the product as a yellow solid (480 mg, 35%).

Following general procedure D, the above-obtained product (100 mg, 0.36 mmol) was reacted with methyl chloroformate (37 μL, 0.48 mmol) and DIPEA (128 μL, 0.72 mmol) in DCM (2 mL) at room temperature for 1 h, giving compound **16a** as a white solid after purification by flash chromatography (PE/EA, 6/1, v/v) (88 mg, 73%).

Following general procedure C, the above-obtained compound **16a** (88 mg, 0.26 mmol) was deprotected with TFA (0.1 mL) in DCM (1 mL) at room temperature for 2 h. Further following general procedure B, the deprotected product was then reacted with propargyl bromide (32 μL, 0.40 mmol) and DIPEA (94.0 μL, 0.53 mmol) in DMF (2 mL) at 65 °C for 3 h. Purification by flash chromatography (PE/EA, 10/1, v/v) gave compound **17** as pale yellow oil (45 mg, 63% over two steps). ^{1}H NMR (300 MHz, $CDCl_3$): δ 7.70 (s, 1H), 6.82−6.88 (m, 2H), 6.55 (s, 1H), 4.03 (s, 2H), 3.95 (d, *J* = 2.1 Hz, 2H), 3.77 (s, 3H), 2.23 (t, *J* = 2.1 Hz, 1H).

*Methyl (4-((4-Fluorobenzyl) (prop-2-yn-1-yl)amino)-2-(trifluoromethyl)phenyl)carbamate (**L3-10**).* Following general procedure B, compound **17** (45 mg, 0.17 mmol) was reacted with *p*-fluorobenzyl bromide (36 μL, 0.27 mmmol) and DIPEA (57μL, 0.33 mmol) in DMF (2 mL) at 65 °C for 3 h. Purification by flash chromatography (PE/EA, 10/1, v/v) gave title compound **L3-10** as pale yellow oil (45 mg, 71%). ^{1}H NMR (300 MHz, $CDCl_3$): δ 7.73 (d, *J* = 7.5 Hz, 1H), 7.25−7.29 (m, 2H), 6.99−7.08 (m, 4H), 6.58 (s, 1H), 4.50 (s, 2H), 4.00 (d, *J* = 2.1 Hz, 2H), 3.68 (s, 3H), 2.54 (t, *J* = 2.1 Hz, 1H); ^{13}C NMR (125 MHz, $CDCl_3$): δ 163.43, 160.99, 154.69, 145.45, 133.16, 128.88, 126.11, 125.28, 122.56, 118.48, 115.75, 111.65, 78.62, 72.97, 54.61, 52.59, 40.23; HRMS (TOF ESI) *m*/*z*: calcd for $C_{19}H_{17}F_4N_2O_2$ $[M + H]^+$, 381.1226; found, 381.1221; HPLC purity: 99.5%.

*Methyl (2-Cyano-4-((4-fluorobenzyl)amino)phenyl)carbamate (**18**).* Following procedures similar to that described to prepare compound **16a**, starting from 2-amino-5-nitrobenzonitrile **5h** (820 mg, 5.0 mmol), compound **16b** was prepared as a yellow solid after purification by flash chromatography (PE/EA, 6/1, v/v) (210 mg, 63% over three steps).

Following general procedure C, the above-obtained compound **16b** (210 mg, 0.72 mmol) was deprotected with TFA (0.1 mL) in DCM (1 mL) at room temperature for 2 h. Following general procedure B, the deprotected product was further reacted with *p*-fluorobenzyl bromide (134 μL, 1.0 mmol) and DIPEA (256 μL, 1.46 mmol) in DMF (2 mL) at 65 °C overnight. Purification by flash chromatography (PE/EA, 8/1, v/v) gave compound **18** as a pale yellow solid (120 mg, 56% over two steps). ^{1}H NMR (300 MHz, $CDCl_3$): δ 7.70 (d, *J* = 8.7 Hz, 1H), 7.26−7.32 (m, 2H), 7.04 (t, *J* = 8.7 Hz, 2H), 6.82 (dd, *J* = 8.4, 2.7 Hz, 2H), 6.70 (d, *J* = 2.7 Hz, 1H), 4.27 (s, 2H), 4.21 (s, 1H), 3.78 (s, 3H).

*Methyl (2-Cyano-4-((4-fluorobenzyl) (prop-2-yn-1-yl)amino)-phenyl)carbamate (**L3-11**).* Following general procedure B, compound **18** (120 mg, 0.40 mmol) was reacted with propargyl bromide (48 μL, 0.62 mmmol) and DIPEA (141 μL, 0.81 mmol) in DMF (2 mL) at 65 °C for 3 h. Purification by flash chromatography (PE/EA, 10/1, v/v) gave title compound **L3-11** as pale yellow oil (85 mg, 63%). ^{1}H NMR (300 MHz, $CDCl_3$): δ 7.70 (d, *J* = 2.1 Hz, 1H), 7.42−7.52 (m, 3H), 7.31 (d, *J* = 9.0 Hz, 1H), 7.02 (t, *J* = 8.7 Hz, 2H), 6.68 (s, 1H), 4.34 (s, 2H), 3.83 (d, *J* = 2.1 Hz, 2H), 3.78 (s, 3H), 2.31 (t, *J* = 2.1 Hz, 1H); ^{13}C NMR (125 MHz, $CDCl_3$): δ 162.69, 161.06, 153.37, 148.94, 132.02, 129.99, 122.52, 117.09, 115.04, 108.22, 77.58, 73.93, 55.16, 52.22, 41.64; HRMS (TOF ERI) *m*/*z*: calcd for $C_{19}H_{16}FN_3NaO_2$ $[M + Na]^+$: 360.1124; found, 360.1114; HPLC purity: 98.7%.

*tert-Butyl (3-Cyano-4-((4-fluorobenzyl) (prop-2-yn-1-yl)amino)-phenyl)carbamate (**20**).* Following method A of general procedure F and general procedure E, respectively, starting material 2-amino-5-nitrobenzonitrile **5i** (820 mg, 5.0 mmol) was hydrogenated in EA (30 mL) using 10% Pd/C (38 mg) as a catalyst to give 2,5-diaminobenzonitrile in a quantitative yield, which was further reacted in DCM (40 mL) with Boc_2O (1.10 g, 5.0 mmol), TEA (0.84 mL, 6.0 mmol), and DMAP (61 mg, 0.5 mmol) at room temperature overnight. Purification by flash chromatography (PE/EA, 10/1, v/v) gave compound **19** as a pale yellow solid (0.87 g, 75% over two steps).

Following general procedure A, the above-obtained compound **19** (200 mg, 0.86 mmol) was condensed with *p*-fluorobenzaldehyde (0.18 mL, 1.68 mmol) in toluene (10 mL) catalyzed by *p*-TsOH (3.7 mg, 0.02 mmol), followed by reduction by $NaBH_4$ (98 mg, 2.58 mmol) in MeOH (10 mL). Purification by flash chromatography (PE/EA, 8/1, 6/1, v/v) gave a yellow solid (243 mg, 83%).

Following general procedure B, the above-obtained solid (243 mg, 0.71 mmol) was reacted with propargyl bromide (85 μL, 1.08 mmol) and DIPEA (253 μL, 1.45 mmol) in DMF (2 mL) at 65 °C for 3 h. Flash chromatography (PE/EA, 10/1, v/v) gave title compound **20** as pale yellow oil (195 mg, 73%). ^{1}H NMR (300 MHz, $CDCl_3$): δ 7.71 (d, *J* = 2.7 Hz, 1H), 7.42−7.47 (m, 2H), 7.26−7.33 (m, 2H), 7.04 (t, *J* = 8.4 Hz, 2H), 6.54 (s, 1H), 4.32 (s, 2H), 3.81 (d, *J* = 2.1 Hz, 2H), 3.77 (s, 3H), 2.27 (t, *J* = 2.1 Hz, 1H), 1.51 (s, 9H).

*Methyl (3-Cyano-4-((4-fluorobenzyl) (prop-2-yn-1-yl)amino)-phenyl)carbamate (**L3-12**).* Following general procedure C, compound **20** (195 mg, 0.51 mmol) was deprotected using TFA (0.1 mL) in DCM (1 mL) at room temperature for 2 h. Following general procedure D, the deprotected amine was then reacted in DCM (2 mL) with methyl chloroformate (60 μL, 0.78 mmol) and DIPEA (185 μL, 1.06 mmol) at room temperature for 1 h. Further purification by flash chromatography (PE/EA, 6/1, v/v) gave title compound **L3-12** as a white solid (163 mg, 94% over two steps). ^{1}H NMR (300 MHz, $CDCl_3$): δ 7.92 (d, *J* = 8.7 Hz, 1H), 7.23−7.28 (m, 2H), 7.10 (dd, *J* = 9.3, 3.0 Hz, 1H), 6.99−7.06 (m, 3H), 6.86 (s, 1H), 4.47 (s, 2H), 3.98 (d, *J* = 2.1 Hz, 2H), 3.79 (s, 3H), 2.27 (t, *J* = 2.1 Hz, 1H); ^{13}C NMR (125 MHz, $CDCl_3$): δ 162.61, 160.98, 153.43, 144.31, 132.34, 128.33, 120.29, 116.47, 115.34, 77.91, 72.71, 54.20, 52.29, 39.88; HRMS (TOF ESI) *m*/*z*: calcd for $C_{19}H_{16}FN_3NaO_2$ $[M + Na]^+$: 360.1124; found, 360.1116; HPLC purity: 98.5%.

*Methyl (4-((4-Fluorobenzyl) (prop-2-yn-1-yl)amino)-2-(trifluoromethoxy)phenyl)carbamate (**L3-13**).* Following general procedure E, 4-bromo-2-(trifluoromethoxy)aniline **5j** (1.28 g, 5.0 mmol) was reacted DCM (40 mL) with Boc_2O (2.4 g, 11.0 mmol), TEA (0.84 mL, 6.0 mmol) and DMAP (0.73 g, 6.0 mmol) at room

https://doi.org/10.1021/acs.jmedchem.0c02252
J. Med. Chem. 2021, 64, 5816−5837

temperature overnight. Purification by flash chromatography (PE/EA, 15/1, v/v) gave compound **21** as a white solid (1.48 g, 65%).

Under a nitrogen atmosphere, to a mixture of compound **21** (0.91 g, 2.0 mmol), *p*-fluorobenzyl amine (344 μL, 3.0 mmol), Cs_2CO_3 (1.3 g, 4.0 mmol), and BINAP (62 mg, 0.1 mmol) in dry toluene (20 mL) was added Pd $(dba)_2$ (92 mg, 10.1 mmol) quickly. The resulting mixture was heated to reflux for 6 h, cooled to room temperature, and added EA (30 mL). Then, the mixture was washed with water, brine, dried over anhydrous Na_2SO_4, filtered, and concentrated in vacuo. The obtained residue was purified by flash chromatography (PE/EA, 10/1, v/v) to give compound **22** as a yellow solid (730 mg, 73%). ^{1}H NMR (300 MHz, $CDCl_3$): δ 7.32 (d, J = 8.7 Hz, 2H), 7.03 (t, J = 8.7 Hz, 2H), 6.96 (d, J = 8.7 Hz, 1H), 6.45−6.49 (m, 3H), 4.28 (d, J = 5.4 Hz, 2H), 4.22 (t, J = 5.4 Hz, 1H), 1.4 (s, 18H); MS (ESI) m/z: 500.2 $[M + H]^+$.

Following general procedure B, compound **22** (250 mg, 0.5 mmol) was reacted with propargyl bromide (58 μL, 0.75 mmol) and DIPEA (177 μL, 1.0 mmol) in DMF (2 mL) at 65 °C for 3 h, giving a white solid after purification by flash chromatography (PE/EA, 10/1, v/v) (223 mg, 83%).

Following general procedure C, the above-obtained solid (223 mg, 0.41 mmol) was deprotected using TFA (0.2 mL) in DCM (2 mL) at room temperature for 2 h. The deprotected amine was then reacted in DCM (2 mL) using methyl chloroformate (48 μL, 0.62 mmol) and DIPEA (150 μL, 0.86 mmol) at room temperature for 1 h, following general procedure D. Further purification by flash chromatography (PE/EA, 8/1, v/v) gave final compound **L3-13** as a white solid (150 mg, 92% over two steps). ^{1}H NMR (300 MHz, $CDCl_3$): δ 7.92 (br s, 1H), 7.25−7.30 (m, 2H), 7.03 (d, J = 8.7 Hz, 2H), 6.81 (dd, J = 8.7, 2.7 Hz, 1H), 6.77 (s, 1H), 6.63 (s, 1H), 4.46 (s, 2H), 3.96 (d, J = 2.1 Hz, 2H), 3.78 (s, 3H), 2.26 (t, J = 2.1 Hz, 1H); ^{13}C NMR (125 MHz, $CDCl_3$): δ 163.15, 161.20, 154.07, 133.25, 128.89, 121.93, 119.52, 115.65, 113.87, 107.66, 78.66, 72.85, 54.78, 52.49, 40.38; HRMS (TOF ESI) m/z: calcd for $C_{19}H_{17}F_4N_2O_3$ $[M + H]^+$, 397.1175, found, 397.1169; HPLC purity: 99.7%.

*Methyl (4-((4-Fluorobenzyl) (prop-2-yn-1-yl)amino)-2,6-dimethylphenyl)carbamate (**L3-14**).* Following general procedure E, 2,6-dimethyl-4-nitroaniline **5k** (0.98 g, 5.9 mmol) was reacted with Boc_2O (2.58 g, 11.8 mmol), TEA (1.77 mL, 12.7 mmol), and DMAP (722 mg, 5.9 mmol) in DCM (40 mL) at room temperature overnight. Purification by flash chromatography (PE/EA, 6/1, v/v) gave the protected product as a pale yellow solid (1.84 g, 85%).

Following method a of general procedure F, the above-obtained solid (1.84 g, 5.0 mmol) was hydrogenated in EA (20 mL) using 10% Pd/C (55 mg) as a catalyst, giving compound **23** in a quantitative yield. ^{1}H NMR (300 MHz, $CDCl_3$): δ 6.38 (s, 1H), 3.52 (s, 2H), 2.05 (s, 6H), 1.39 (s, 18H).

Following general procedure A, the above-obtained compound **23** (336 mg, 1.0 mmol) was condensed with *p*-fluorobenzaldehyde (108 μL, 1.0 mmol) in toluene (10 mL) catalyzed by *p*-TsOH (4.3 mg, 0.025 mmol) after reflux for 3 h, followed by reduction by $NaBH_4$ (76 mg, 2.0 mmol) in MeOH (20 mL) at room temperature for 2 h, giving the product as a yellow solid after flash chromatography (PE/EA, 10/1, v/v) (320 mg, 72%).

Following general procedure B, the above-obtained compound (320 mg, 0.72 mmol) was reacted with propargyl bromide (84 μL, 1.08 mmol) and DIPEA (257 μL, 1.47 mmol) in DMF (5 mL) at 65 °C for 4 h. Purification by flash chromatography (PE/EA, 15/1, v/v) gave intermediate **24** (312 mg, 90%).

Following general procedure C, intermediate **24** (48 mg, 0.1 mmol) was deprotected using TFA (0.1 mL) in DCM (1 mL) at room temperature for 2 h. The deprotected product was then reacted in DCM (1 mL) with methyl chloroformate (11.7 μL, 0.15 mmol) and DIPEA (35 μL, 0.20 mmol) at room temperature for 1 h, following general procedure D. Further purification by flash chromatography (PE/EA, 8/1, v/v) gave final compound **L3-14** as a white solid (31 mg, 91%).^{1}H NMR (300 MHz, $CDCl_3$): δ 7.27 (dd, J = 8.4, 5.4 Hz, 2H), 7.02 (t, J = 9.0 Hz, 2H), 6.63 (s, 2H), 5.95 (br s, 1H), 4.49 (s, 2H), 3.98 (d, J = 2.1 Hz, 2H), 3.74 (br s, 3H), 2.25 (t, J = 2.1 Hz, 1H), 2.21 (s, 6H); ^{13}C NMR (125 MHz, $CDCl_3$): δ 163.85, 160.60, 155.67, 147.75, 137.12, 134.15, 128.99, 125.13, 115.74, 114.11, 798.66, 72.49, 54.43, 52.54, 39.90, 18.94; HRMS (TOF ESI) m/z: calcd for $C_{20}H_{22}FN_2O_2$ $[M + H]^+$, 341.1665; found, 341.1656; HPLC purity: 99.5%.

*Methyl (4-((4-Fluorobenzyl) (prop-2-yn-1-yl)amino)-3,5-dimethylphenyl)carbamate (**L3-15**).* Following general procedure D, compound **23** (336 mg, 1.0 mmol) was reacted with methyl chloroformate (117 μL, 1.5 mmol) and DIPEA (350 μL, 2.0 mmol) in DCM (1 mL) at room temperature for 1 h, giving intermediate **25** as pale yellow oil after purification by flash chromatography (PE/EA, 8/1, v/v) (374 mg, 95%).

Following general procedure C, intermediate **25** (374 mg, 0.95 mmol) was deprotected using TFA (0.2 mL) in DCM (2 mL) at room temperature for 2 h. The deprotected product was then reacted with *p*-fluorobenzyl bromide (128 μL, 0.95 mmol) and DIPEA (0.34 mL, 2.0 mmol) in DMF (3 mL) at 65 °C for 4 h. Purification by flash chromatography (PE/EA, 10/1, v/v) gave compound **26** as pale yellow oil (192 mg, 67%). ^{1}H NMR (300 MHz, $CDCl_3$): δ 7.78 (br s, 1H), 7.26 (m, 1H), 7.02 (t, J = 8.4 Hz, 2H), 6.64 (m, 2H), 6.51 (br s, 1H), 4.45 (s, 2H), 3.95 (d, J = 2.1 Hz, 2H), 3.77 (s, 3H), 2.24 (t, J = 2.1 Hz, 1H).

Following general procedure B, compound **26** (192 mg, 0.64 mmol) was further reacted with propargyl bromide (50 μL, 0.64 mmol) and DIPEA (226 μL, 1.3 mmol) in DMF (3 mL) at 65 °C for 4 h. Purification by flash chromatography (PE/EA, 15/1, v/v) gave compound **L3-15** as a white solid (165 mg, 76%). ^{1}H NMR (300 MHz, $CDCl_3$): δ 7.36 (d, J = 8.7 Hz, 2H), 7.04 (s, 2H), 6.91 (t, J = 9.0 Hz, 3H), 4.48 (s, 2H), 4.20 (s, 2H), 3.75 (s, 3H), 2.23−2.38 (m, 7H); ^{13}C NMR (125 MHz, $CDCl_3$): δ 163.27, 160.83, 154.16, 143.39, 138.10, 135.05, 130.47, 119.19, 115.18, 114.97, 81.52, 72.02, 56.06, 52.29, 41.21, 19.92; HRMS (TOF ESI) m/z: calcd for $C_{20}H_{22}FN_2O_2$ $[M + H]^+$, 341.1665; found, 341.1659; HPLC purity: 95.1%.

Plasmid Construction. The plasmids encoding human KCNQ1, rat KCNQ2, rat KCNQ3, human KCNQ4, and human KCNQ5 were gifts from Drs. T. Jentsch (Zentrum für Molekulare Neurobiologie, Hamburg, Germany), D. MacKinnon (State University of New York, Stony Brook, NY), M. Sanguinetti (University of Utah, Salt Lake City, UT), M. Shapiro (University of Texas Health Science Center, San Antonio, TX), and Kenneth L. Byron (Loyola University, Chicago, IL), respectively. In addition, the EGFP were offered by Haijun Chen (State University of New York, Stony Brook, NY). A278T mutation of rKCNQ3 (AF091247) were introduced using the QuikChange II site-directed mutagenesis kit (Stratagene).

Cell Culture and Transient Transfection. Chinese hamster ovary (CHO) cells were cultured in DMEM/F12 (Gibco, Life Technologies, Carlsbad, CA, USA) with 10% FBS. 24 h prior to transfection, cells were split into 6-well dishes. Plasmids of EGFP and KCNQ channels were cotransfected with Lipofectamine 3000 reagent (Invitrogen, Life Technologies, Carlsbad, CA, USA) according to the manufacturer's instructions. Moreover, to express KCNQ2/KCNQ3 channels, the cDNA ratio transfected is 1:1.

Electrophysiology. A standard whole-cell recording was performed at room temperature in CHO cells with an Axopathca-200B amplifier (Molecular Devices, Sunnyvale, CA). The pipettes were pulled from borosilicate glass capillaries (World Precision Instruments, Sarasota, FL) and had resistances of 3−5 MΩ when filled with the intracellular solution. The holding potential is −80 mV, followed by a series of depolarization steps from −90 to +60 mV with a 10 mV increment, the currents were measured at the end of depolarization to −10 mV to determine I/I_0, and the tail currents elicited at −120 mV were measured to obtain $\Delta V_{1/2}$. The intracellular solution contained 145 mM KCl, 1 mM $MgCl_2$, 5 mM EGTA, 10 mM HEPES and 5mM MgATP (pH = 7.3), and the extracellular solution contained 140 mM NaCl, 5 mM KCl, 2 mM $CaCl_2$, 1.5 mM $MgCl_2$, 10 mM Glucose (pH = 7.4), and 10 mM HEPES. During the recording, constant perfusion of the extracellular solution was maintained using a bath perfusion system (ALA Scientific Instruments, NY). The electrical signals were filtered at 1 kHz and digitized using a DigiData 1322A with pClamp 9.2 software (Molecular

https://doi.org/10.1021/acs.jmedchem.0c02252
J. Med. Chem. 2021, 64, 5816−5837

Devices, Sunnyvale, CA). Series resistance was compensated by 60−80%.

Patch Clamp Data Analysis. Patch clamp data were processed using Clampfit 10.2 (Molecular Devices, Sunnyvale, CA, USA) and then analyzed in GraphPad Prism 8 (GraphPad Software, San Diego, CA, USA). Voltage-dependent activation curves were fitted using the Boltzmann equation, $G = G_{min} + (G_{max} - G_{min})/(1 + \exp(V - V_{1/2})/S)$, where G_{max} is the maximum conductance, G_{min} is the minimum conductance, $V_{1/2}$ is the voltage for reaching 50% of maximum conductance, and S is the slope factor. Dose−response curves were fitted with the Hill equation, $E = E_{max}/(1 - (EC_{50}/C)\ P)$, where EC_{50} is the drug concentration producing half of the maximum response and P is the Hill coefficient. The data are presented as the mean ± SEM.

Use of Animals. In the present study, healthy male Chinese Kun Ming (KM) mice (18−24 g) from Beijing HFK Bioscience (Beijing, China), male C57BL/6 mice (20−25 g) obtained from Shanghai Slac Laboratory Animal (Shanghai, China), and healthy male Sprague Dawley (SD) rats (180−220 g) provided by Shanghai Sippr-Bk Laboratory Animal (Shanghai, China) were used. Animals were group housed in a temperature (22−24 °C) and relative humidity (50−70%) controlled facility and maintained on a constant 12 h light/dark cycle with free access to food and water. This study was approved by the Animal Care and Use Committee of Shanghai Institute of Materia Medica, Chinese Academy of Sciences (IACUC Numbers: 2016-04-JHL-13 and 2020-02-GZB-05) and performed in compliance with the National Institutes of Health Guide for the Care and Use of Laboratory Animals.

Pharmacokinetic Studies. PK studies were performed in KM mice. The mice were fasted for 12 h before and 2 h after drug administration. The test compound **HN37** was prepared for an oral formulation using 5% DMSO/5% Tween 80/90% normal saline, and the oral formulation was diluted with normal saline containing 1% Tween 80 to obtain the intravenous formulation. Mice ($n = 3$ per time point) were given **HN37** orally at 5 mg/kg or intravenously at 2 mg/kg. Blood samples (0.5 mL) were collected at 0.25, 0.5, 1, 2, 4, 6, 8, and 24 h from the abdominal aorta into the heparinized tubes after oral dosing, or blood samples (0.2 mL) were collected from the posterior venous plexus of the eyeball at 0.083, 0.25, 0.5, 1, 2, 4, 6, 8, and 24 h after iv injection. The plasma was separated by centrifugation (11,000 rpm for 5 min) and then stored at −80 °C until analyzed. Mice treated orally were sacrificed to obtain the whole brain tissue which was also stored at −80 °C. Plasma samples (20 μL) were treated with the addition of the internal standard solution (20 μL) and acetonitrile (300 μL), then vortexed for 15 min (1000 rpm, RT), and centrifuged of 15 min (3700 rpm, 4 °C). The supernatants were collected for analysis. The whole brain samples were homogenized in acetonitrile with a 10-fold volume to tissue weight (8000 rpm, 3 × 30 s), then was sonicated for 5 min. The obtained homogenate was then treated as described for the plasma samples. The plasma and brain levels of compound **HN37** were analyzed using LC−MS/MS. The data were processed using Analyst software version 1.6.3 (Sciex, Ontario, Canada). PK studies of **HN37** were also carried out in SD rats at the oral doses of 2, 6, and 20 mg/kg, and the procedure was performed similarly as in the mice.

To examine the plasma and brain exposures after the oral administration of compound **HN37** and RTG, the separate PK studies were performed in the MES test and rotarod test in KM mice. Upon the completion of the MES test or rotarod test, mice treated with **HN37** and RTG were sacrificed to collect brain and plasma samples, and the brain and plasma concentrations of compound **HN37** were measured as described above. For compound RTG, the brain samples were processed and analyzed the same as **HN37**, and the plasma samples were slightly different. After centrifugation with the internal standard solution and acetonitrile for plasma samples, the supernatants (20 μL) were added into 1:1 acetonitrile/water (v/v) for 15 min of vertexing to obtain a mixture for analysis by LC−MS/MS.

Time-Dependent Inhibition Potential Assay. To determine whether **HN37** was a time-dependent inhibitor of major human hepatic CYP enzymes, human liver microsomes were used to evaluate the time-dependent inhibition potential of **HN37** on cytochrome P450s. Human liver microsomes was pre-incubated with **HN37** at various concentrations (0.10−50 μM) for 0.5 h with the presence or absence of NADPH, followed by the addition of specific CYP450 probe substrates and further incubation. An LC−MS/MS method was used to determine the concentration of each specific metabolite and the value of IC_{50} was calculated to indicate the potential of TDI of **HN37** toward major CYP450. The percent of enzyme activity remaining after incubation with **HN37** is calculated by the following equations

$$\%\ \text{activity remaining (at appointed conc.)} = \frac{\text{metabolite conc. at appointed conc. of test compound}}{\text{metabolite conc. without test compound}} \times 100\%$$

The concentration of **HN37** inhibited the metabolism of the respective P450 probe substrates by 50% was determined as $IC_{50NADPH^-}/IC_{50NADPH^+}$ calculated using the Probit model by GraphPad Prism 8.0.1 software.

Anticonvulsant Efficacy. The anticonvulsant efficacy of compound **HN37** was evaluated in MES, sc-PTZ, and 6 Hz tests. All test compounds including retigabine, topiramate, and levetiracetam as references, were freshly suspended in 0.5% CMC-Na and administered intragastrically to mice in a volume of 20 mL/kg body weight and in a volume of 10 mL/kg body weight orally to rats 0.5 or 1 h before the seizure tests. The pentylenetetrazol solution was prepared freshly and dissolved in normal saline.

Maximal Electroshock Seizure Test in mice and Rats. In this anticonvulsant screening test, the mouse test procedure was described in our previous papers,[41,58] and the rat test was performed partly according to the method introduced by Swinyard.[59] In the mouse test, a stimulus intensity of 160 V was applied through ear clip electrodes for 5.4 s using an electronic stimulator (YLS-9A, Bio-will, Shanghai, China). In the rat test, the seizures were induced by an electronic stimulator (EC-02, Orchid Scientifics, Maharashtra, India) by the delivery of a 200 mA current to the cornea for 0.2 s. Both electroshock applications caused immediate hindlimb tonic extension. The test compound which showed a complete suppression of the hindlimb tonic seizure was thought to have a protective effect in the MES test. Compound **HN37** and the reference drugs were determined by the anticonvulsant quantification study. Eight to ten KM mice or SD rats were used per group per dose, and 5−6 doses were used to establish the median effective dose (ED_{50}), which were calculated by nonlinear regression using Graph Pad Prism 5. After completion of the test, all mice that were treated with HN37 and RTG were sacrificed immediately, and the brain and plasma sample collection, processing, and analysis, were performed according to the above methods in the PK studies in mice.

Subcutaneous Pentylenetetrazol Test in Mice. PTZ was injected subcutaneously to KM mice at a dose of 100 mg/kg in a volume of 10 mL/kg body weight, and this dose induced clonic and tonic seizures first, and then led to death in mice in our previous study.[56,60] The number and the latency of clonic seizures, tonic seizures, and death were recorded within 1 h after PTZ injection, respectively. The mice not displaying both clonic and tonic seizures were considered to be protected. Ten mice were used per group per dose. Compound **HN37** and reference drugs were evaluated in this test and the ED_{50} calculation was the same with the MES test.

6 Hz Psychomotor Seizure Test in Mice. 6 Hz psychomotor seizure was considered as the only acute model of drug-resistant epilepsy,[61] and this test was performed as previously described.[56,60] The C57BL/6 mice were chosen and were stimulated through corneal electrodes using a Grass stimulator (S48, Grass technologies, USA) connected to a constant current unit (CCU1, Grass technologies, USA). Focal seizures were induced by delivering a stimulus of 32 or 44 mA current (6 Hz, 0.2 ms rectangular pulse width) for 3 s duration. The mice exhibited immobility associated with rearing, automatisms, forelimb clonus, twitching of the vibrissae, and Straub

https://doi.org/10.1021/acs.jmedchem.0c02252
J. Med. Chem. 2021, 64, 5816−5837

tail for 10−50 s duration following the electrical stimulation. The mice resuming normal behavior within 7 s from the stimulation were considered protected. There were ten mice per group per dose. The determination of ED_{50} values for **HN37** and reference drugs was performed as above.

Neurotoxicity in Mice. To assess the neurotoxicity effects for compound **HN37** and reference drugs, the standardized rotarod test was performed in KM or C57BL/6 mice. The mice were placed on a rotarod appliance (YLS-4C, Bio-will, Shanghai, China) with a rod of 3 cm diameter, rotating at a constant speed of 6 rpm. The day before the compound test, all the mice were pre-trained and only the animals able to remain on the rod for at least 1 min every time in three consecutive trials (3 min) were retained. On the test day, the mice were measured in the rotarod test at 1 h after oral gavage administration of **HN37** and reference drugs, respectively. The animal unable to remain on the rod for 3 consecutive periods was considered motor coordination impaired. Six to ten mice were used per group per dose, and 4−6 doses were used to establish the median neurotoxic dose (TD_{50}) determined by nonlinear regression using Graph Pad Prism 5. To determine the safety margin for **HN37**, the plasma and brain exposures of **HN37** and RTG were also detected as described in PK studies following the finishing of the test.

■ ASSOCIATED CONTENT

Supporting Information

The Supporting Information is available free of charge at https://pubs.acs.org/doi/10.1021/acs.jmedchem.0c02252.

Additional information for the CYP inhibition study and TDI assessment, time effect of **HN37** in the mouse MES test, quantitative anticonvulsant effects of **HN37** and RTG in rat MES test, and NMR and HPLC spectra for final compounds (PDF)

Molecular formula strings for all the final compounds (CSV).

■ AUTHOR INFORMATION

Corresponding Authors

Zhao-Bing Gao − *Chinese National Center for Drug Screening, CAS Key Laboratory of Receptor Research, State Key Laboratory of Drug Research, Shanghai Institute of Materia Medica, Chinese Academy of Sciences, Shanghai 201203, China; School of Chinese Materia Medica, Nanjing University of Chinese Medicine, Nanjing City, Jiangsu 210023, China*; Email: zbgao@simm.ac.cn

Fa-Jun Nan − *Chinese National Center for Drug Screening, CAS Key Laboratory of Receptor Research, State Key Laboratory of Drug Research, Shanghai Institute of Materia Medica, Chinese Academy of Sciences, Shanghai 201203, China; Yantai Key Laboratory of Nanomedicine & Advanced Preparations, Yantai Institute of Materia Medica, Yantai City, Shandong 264000, China*; orcid.org/0000-0002-2284-3637; Email: fjnan@simm.ac.cn

Authors

Yang-Ming Zhang − *Chinese National Center for Drug Screening, CAS Key Laboratory of Receptor Research, State Key Laboratory of Drug Research, Shanghai Institute of Materia Medica, Chinese Academy of Sciences, Shanghai 201203, China; Yantai Key Laboratory of Nanomedicine & Advanced Preparations, Yantai Institute of Materia Medica, Yantai City, Shandong 264000, China*

Hai-Yan Xu − *School of Chinese Materia Medica, Nanjing University of Chinese Medicine, Nanjing City, Jiangsu 210023, China; Chinese National Center for Drug Screening, CAS Key Laboratory of Receptor Research, State Key Laboratory of Drug Research, Shanghai Institute of Materia Medica, Chinese Academy of Sciences, Shanghai 201203, China*

Hai-Ning Hu − *Chinese National Center for Drug Screening, CAS Key Laboratory of Receptor Research, State Key Laboratory of Drug Research, Shanghai Institute of Materia Medica, Chinese Academy of Sciences, Shanghai 201203, China*

Fu-Yun Tian − *Chinese National Center for Drug Screening, CAS Key Laboratory of Receptor Research, State Key Laboratory of Drug Research, Shanghai Institute of Materia Medica, Chinese Academy of Sciences, Shanghai 201203, China*

Fei Chen − *Chinese National Center for Drug Screening, CAS Key Laboratory of Receptor Research, State Key Laboratory of Drug Research, Shanghai Institute of Materia Medica, Chinese Academy of Sciences, Shanghai 201203, China*

Hua-Nan Liu − *Chinese National Center for Drug Screening, CAS Key Laboratory of Receptor Research, State Key Laboratory of Drug Research, Shanghai Institute of Materia Medica, Chinese Academy of Sciences, Shanghai 201203, China*

Li Zhan − *Chinese National Center for Drug Screening, CAS Key Laboratory of Receptor Research, State Key Laboratory of Drug Research, Shanghai Institute of Materia Medica, Chinese Academy of Sciences, Shanghai 201203, China*

Xiao-Ping Pi − *Chinese National Center for Drug Screening, CAS Key Laboratory of Receptor Research, State Key Laboratory of Drug Research, Shanghai Institute of Materia Medica, Chinese Academy of Sciences, Shanghai 201203, China*

Jie Liu − *Hainan Haiyao Company Ltd., Haikou City, Hainan 570311, China*

Complete contact information is available at: https://pubs.acs.org/10.1021/acs.jmedchem.0c02252

Author Contributions

⊥Y.-M.Z., H.-Y.X., and H.-N.H contributed equally.

Notes

The authors declare no competing financial interest.

■ ACKNOWLEDGMENTS

This work was supported by grants from The National Natural Science Foundation of China (81825021), the National Science and Technology Major Project (2013ZX09103-001-016 and 2018ZX09711002-013-002), Chinese Academy of Sciences (XDA12040211 and CASIMM0120151001), Ministry of Science and Technology of China (2013CB910604), and Shanghai Science and Technology Committee (16431901700 and 19431906000). The authors are grateful to J-L Zhou for TDI assessment and discussion. The authors thank Y-F Zhang and Z-W Gao for their suggestions and discussions about the PK study.

■ ABBREVIATIONS

AED, antiepileptic drug; P-RTG, ethyl *N*-[2-amino-4-((4-fluorobenzyl) (prop-2-ynyl)amino)phenyl] carbamate; CNS, central nervous system; Kv, voltage-gated potassium channel; EC_{50}, median effective concentration; IC_{50}, half-maximal inhibitory concentration; ED_{50}, median effective dose; TD_{50}, median neurotoxic dose; DCM, dichloromethane; DIPEA, *N*,*N*-diisopropylethylamine; DMF, *N*,*N*-dimethylformamide;

THF, tetrahydrofuran; TFA, trifluoroacetic acid; TEA, triethyl amine; DMAP, 4-dimethylaminopyridine; MES, maximal electroshock; scPTZ, subcutaneous pentylenetetrazol; EMA, European Medicines Agency; FDA, Food and Drug Administration; NMPA, National Medical Products Administration

REFERENCES

(1) WHO. Epilepsy, 2020 April. Available from: https://www.who.int/en/news-room/fact-sheets/detail/epilepsy (accessed 20 June 2019).

(2) Chong, D. J.; Bazil, C. W. Update on anticonvulsant drugs. *Curr. Neurol. Neurosci. Rep.* **2010**, *10*, 308−318.

(3) Chong, D. J.; Lerman, A. M. Practice update: Review of anticonvulsant therapy. *Curr. Neurol. Neurosci. Rep.* **2016**, *16*, 39.

(4) Schulze-Bonhage, A. A 2017 review of pharmacotherapy for treating focal epilepsy: Where are we now and how will treatment develop? *Expet Opin. Pharmacother.* **2017**, *18*, 1845−1853.

(5) Younus, I.; Reddy, D. S. A resurging boom in new drugs for epilepsy and brain disorders. *Expet Rev. Clin. Pharmacol.* **2018**, *11*, 27−45.

(6) Vossler, D. G.; Yilmaz, U. Ezogabine treatment of childhood absence epilepsy. *Epileptic Disord.* **2014**, *16*, 121−124.

(7) Jentsch, T. J. Neuronal KCNQ potassium channels:physislogy and role in disease. *Nat. Rev. Neurosci.* **2000**, *1*, 21−30.

(8) Stafstrom, C. E.; Grippon, S.; Kirkpatrick, P. Ezogabine (retigabine). *Nat. Rev. Drug Discovery* **2011**, *10*, 729−730.

(9) Jankovic, S.; Ilickovic, I. The preclinical discovery and development of ezogabine for the treatment of epilepsy. *Expert Opin. Drug Discovery* **2013**, *8*, 1429−1437.

(10) Orhan, G.; Wuttke, T. V.; Nies, A. T.; Schwab, M.; Lerche, H. Retigabine/Ezogabine, a KCNQ/KV7 channel opener: pharmacological and clinical data. *Expet Opin. Pharmacother.* **2012**, *13*, 1807−1816.

(11) Millichap, J. J.; Park, K. L.; Tsuchida, T.; Ben-Zeev, B.; Carmant, L.; Flamini, R.; Joshi, N.; Levisohn, P. M.; Marsh, E.; Nangia, S.; Narayanan, V.; Ortiz-Gonzalez, X. R.; Patterson, M. C.; Pearl, P. L.; Porter, B.; Ramsey, K.; McGinnis, E. L.; Taglialatela, M.; Tracy, M.; Tran, B.; Venkatesan, C.; Weckhuysen, S.; Cooper, E. C. KCNQ2 encephalopathy: Features, mutational hot spots, and ezogabine treatment of 11 patients. *Neurol.: Genet.* **2016**, *2*, No. e96.

(12) Wong, M.; Ciliberto, M.; Weisenberg, J. Clinical utility, safety, and tolerability of ezogabine (retigabine) in the treatment of epilepsy. *Drug Healthc. Patient Saf.* **2012**, *4*, 81−86.

(13) Streng, T.; Christoph, T.; Andersson, K.-E. Urodynamic Effects of the K^+ Channel (Kcnq) Opener Retigabine in Freely Moving, Conscious Rats. *J. Urol.* **2004**, *172*, 2054−2058.

(14) Rode, F.; Svalø, J.; Sheykhzade, M.; Rønn, L. C. B. Functional effects of the KCNQ modulators retigabine and XE991 in the rat urinary bladder. *Eur. J. Pharmacol.* **2010**, *638*, 121−127.

(15) Seefeld, M. A.; Lin, H.; Holenz, J.; Downie, D.; Donovan, B.; Fu, T.; Pasikanti, K.; Zhen, W.; Cato, M.; Chaudhary, K. W.; Brady, P.; Bakshi, T.; Morrow, D.; Rajagopal, S.; Samanta, S. K.; Madhyastha, N.; Kuppusamy, B. M.; Dougherty, R. W.; Bhamidipati, R.; Mohd, Z.; Higgins, G. A.; Chapman, M.; Rouget, C.; Lluel, P.; Matsuoka, Y. Novel KV7 ion channel openers for the treatment of epilepsy and implications for detrusor tissue contraction. *Bioorg. Med. Chem. Lett.* **2018**, *28*, 3793−3797.

(16) Shkolnik, T. G.; Feuerman, H.; Didkovsky, E.; Kaplan, I.; Bergman, R.; Pavlovsky, L.; Hodak, E. Blue-gray mucocutaneous discoloration a new adverse effect of ezogabine. *JAMA Dermatol.* **2014**, *150*, 984−989.

(17) Mathias, S. V.; Abou-Khalil, B. W. Ezogabine skin discoloration is reversible after discontinuation. *Epilepsy Behav. Case Rep.* **2017**, *7*, 61−63.

(18) Clark, S.; Antell, A.; Kaufman, K. New antiepileptic medication linked to blue discoloration of the skin and eyes. *Ther. Adv. Drug Saf.* **2015**, *6*, 15−19.

(19) Beacher, N. G.; Brodie, M. J.; Goodall, C. A case report: retigabine induced oral mucosal dyspigmentation of the hard palate. *BMC Oral Health* **2015**, *15*, 122.

(20) Bock, C.; Link, A. How to replace the lost keys? Strategies toward safer KV7 channel openers. *Future Med. Chem.* **2019**, *11*, 337−355.

(21) Groseclose, M. R.; Castellino, S. An investigation into retigabine (ezogabine) associated dyspigmentation in rat eyes by maldi imaging mass spectrometry. *Chem. Res. Toxicol.* **2019**, *32*, 294−303.

(22) Evans, S.; Saenz, A. A.; Harrington, C.; Kelly, D.; Walsh, N.; McDonald, S.; Lee, W.; Brickel, N. Pigmentary abnormalities (discoloration) associated with ezogabine/retigabine treatment: nonclinical aspects. *Epilepsy Curr.* **2015**, *15*, 336−337. (AES 2014 Annual Meeting Online Abstract Supplement)

(23) Douša, M.; Srbek, J.; Rádl, S.; Černý, J.; Klecán, O.; Havlíček, J.; Tkadlecová, M.; Pekárek, T.; Gibala, P.; Nováková, L. Identification, characterization, synthesis and HPLC quantification of new process-related impurities and degradation products in retigabine. *J. Pharm. Biomed. Anal.* **2014**, *94*, 71−76.

(24) Liu, R.; Tzounopoulos, T.; Wipf, P. Synthesis and Optimization of Kv7 (KCNQ) Potassium Channel Agonists: The Role of Fluorines in Potency and Selectivity. *ACS Med. Chem. Lett.* **2019**, *10*, 929−935.

(25) Shilova, E. A.; Heynderickx, A.; Siri, O. Bandrowski's base revisited: Toward a unprecedented class of quinonediimines or new two-way chromophoric molecular switches. *J. Org. Chem.* **2010**, *75*, 1855−1861.

(26) Methling, K.; Reszka, P.; Lalk, M.; Vrana, O.; Scheuch, E.; Siegmund, W.; Terhaag, B.; Bednarski, P. J. Investigation of the in vitro metabolism of the analgesic flupirtine. *Drug Metab. Dispos.* **2009**, *37*, 479−493.

(27) Wang, L.; Qiao, G.-H.; Hu, H.-N.; Gao, Z.-B.; Nan, F.-J. Discovery of novel retigabine derivatives as potent KCNQ4 and KCNQ5 channel agonists with improved specificity. *ACS Med. Chem. Lett.* **2019**, *10*, 27−33.

(28) Bock, C.; Beirow, K.; Surur, A. S.; Schulig, L.; Bodtke, A.; Bednarski, P. J.; Link, A. Synthesis and potassium KV7 channel opening activity of thioether analogues of the analgesic flupirtine. *Org. Biomol. Chem.* **2018**, *16*, 8695−8699.

(29) Bock, C.; Surur, A. S.; Beirow, K.; Kindermann, M. K.; Schulig, L.; Bodtke, A.; Bednarski, P. J.; Link, A. Sulfide Analogues of Flupirtine and Retigabine with Nanomolar K V 7.2/K V 7.3 Channel Opening Activity. *Chemmedchem* **2019**, *14*, 952−964.

(30) Surur, A. S.; Beirow, K.; Bock, C.; Schulig, L.; Kindermann, M. K.; Bodtke, A.; Siegmund, W.; Bednarski, P. J.; Link, A. Flupirtine Analogues: Explorative Synthesis and Influence of Chemical Structure on KV7.2/KV7.3 Channel Opening Activity. *Chemistryopen* **2019**, *8*, 41−44.

(31) Surur, A. S.; Bock, C.; Beirow, K.; Wurm, K.; Schulig, L.; Kindermann, M. K.; Siegmund, W.; Bednarski, P. J.; Link, A. Flupirtine and retigabine as templates for ligand-based drug design of KV7.2/3 activators. *Org. Biomol. Chem.* **2019**, *17*, 4512−4522.

(32) Ostacolo, C.; Miceli, F.; Di Sarno, V.; Nappi, P.; Iraci, N.; Soldovieri, M. V.; Ciaglia, T.; Ambrosino, P.; Vestuto, V.; Lauritano, A.; Musella, S.; Pepe, G.; Basilicata, M. G.; Manfra, M.; Perinelli, D. R.; Novellino, E.; Bertamino, A.; Gomez-Monterrey, I. M.; Campiglia, P.; Taglialatela, M. Synthesis and pharmacological characterization of conformationally restricted retigabine analogues as novel neuronal Kv7 channel activators. *J. Med. Chem.* **2020**, *63*, 163−185.

(33) Yang, S.; Lu, D.; Ouyang, P. Design, synthesis and evaluation of substituted piperidine based KCNQ openers as novel antiepileptic agents. *Bioorg. Med. Chem. Lett.* **2018**, *28*, 1731−1735.

(34) Yang, S.; Lu, D.; Ouyang, P. Design, synthesis and evaluation of novel N-phenylbutanamide derivatives as KCNQ openers for the treatment of epilepsy. *Bioorg. Med. Chem. Lett.* **2018**, *28*, 3004−3008.

(35) Zhang, F.; Liu, Y.; Tang, F.; Liang, B.; Chen, H.; Zhang, H.; Wang, K. Electrophysiological and pharmacological characterization of a novel and potent neuronal Kv7 channel opener SCR2682 for antiepilepsy. *FASEB J.* **2019**, *33*, 9154−9166.

https://doi.org/10.1021/acs.jmedchem.0c02252
J. Med. Chem. 2021, 64, 5816−5837

(36) Chen, H.; Liang, B.; Zhao, Z.; Cao, W.; Xu, W.; Li, Q.; Wang, J.; Zhang, P.; Jiang, Z.; Zhang, G.; Gao, C.; Gong, H.; Zuo, G. Compound as Potassium Channel Modulator. WO2014048165A1, 2014.
(37) Vernier, J.-M.; De La Rosa, M. A.; Chen, H.; Wu, J. Z.; Larson, G. L.; Cheney, I. W. Derivatives of 4-(N-azacycloalkyl) anilides as Potassium Channel Modulators. US Patent 8,293,911 B2, 2012.
(38) Bialer, M.; Johannessen, S. I.; Koepp, M. J.; Levy, R. H.; Perucca, E.; Tomson, T.; White, H. S. Progress report on new antiepileptic drugs: A summary of the fourteenth eilat conference on new antiepileptic drugs and devices (eilat xiv). I. Drugs in preclinical and early clinical development. *Epilepsia* **2018**, *59*, 1811−1841.
(39) Beatch, G. N. Methods for Enhancing the Bioavailability and Exposure of a Voltage-gated Potassium Channel Opener, WO2019217924A1, 2019.
(40) Nan, F.; Li, M.; Gao, Z.; Chen, F.; Zhang, Y.; Zhou, P.; Hu, H.; Xu, H.; Liu, S. Novel Compound as Kcnq Potassium Channel agonist, Preparation Method Therefor and Use Thereof, WO2013060097A1, 2012.
(41) Zhou, P.; Zhang, Y.; Xu, H.; Chen, F.; Chen, X.; Li, X.; Pi, X.; Wang, L.; Zhan, L.; Nan, F.; Gao, Z. P-retigabine: An N-propargyled retigabine with improved brain distribution and enhanced anti-epileptic activity. *Mol. Pharmacol.* **2015**, *87*, 31−38.
(42) Hanson, A. W.; Röhrl, M. The crystal structure of lidocaine hydrochloride monohydrate. *Acta Crystallogr., Sect. B: Struct. Crystallogr. Cryst. Chem.* **1972**, *28*, 3567−3571.
(43) Hanson, J. R.; Hitchcock, P. B.; Rodriguez-Medina, I. C. The conformation of some disubstituted anilides. *J. Chem. Res.* **2004**, *2004*, 664−666.
(44) Ruetsch, Y.; Boni, T.; Borgeat, A. From cocaine to ropivacaine: the history of local anesthetic drugs. *Curr. Top. Med. Chem.* **2001**, *1*, 175−182.
(45) Gunthorpe, M. J.; Large, C. H.; Sankar, R. The mechanism of action of retigabine (ezogabine), a first-in-class K+ channel opener for the treatment of epilepsy. *Epilepsia* **2012**, *53*, 412−424.
(46) Zhou, P.; Yu, H.; Gu, M.; Nan, F.; Gao, Z.; Li, M. Phosphatidylinositol 4,5-bisphosphate alters pharmacological selectivity for epilepsy-causing KCNQ potassium channels. *Proc. Natl. Acad. Sci. U.S.A.* **2013**, *110*, 8726−8731.
(47) Shapiro, M. S.; Roche, J. P.; Kaftan, E. J.; Cruzblanca, H.; Mackie, K.; Hille, B. Reconstitution of Muscarinic Modulation of the KCNQ2/KCNQ3 K^+Channels that Underlie the Neuronal M Current. *J. Neurosci.* **2000**, *20*, 1710−1721.
(48) Etxeberria, A.; Santana-Castro, I.; Regalado, M. P.; Aivar, P.; Villarroel, A. Three mechanisms underlie KCNQ2/3 heteromeric potassium M-channel potentiation. *J. Neurosci.* **2004**, *24*, 9146−9152.
(49) Greene, D. L.; Hoshi, N. Modulation of Kv7 channels and excitability in the brain. *Cell. Mol. Life Sci.* **2017**, *74*, 495−508.
(50) Munro, G.; Dalby-Brown, W. Kv7 (KCNQ) Channel Modulators and Neuropathic Pain. *J. Med. Chem.* **2007**, *50*, 2576−2582.
(51) Löscher, W. Animal models of seizures and epilepsy: Past, present, and future role for the discovery of antiseizure drugs. *Neurochem. Res.* **2017**, *42*, 1873−1888.
(52) Kehne, J. H.; Klein, B. D.; Raeissi, S.; Sharma, S. The national institute of neurological disorders and stroke (ninds) epilepsy therapy screening program (etsp). *Neurochem. Res.* **2017**, *42*, 1894−1903.
(53) Krall, R. L.; Penry, J. K.; White, B. G.; Kupferberg, H. J.; Swinyard, E. A. Antiepileptic Drug Development: II. Anticonvulsant Drug Screening. *Epilepsia* **1978**, *19*, 409−428.
(54) Löscher, W. Critical review of current animal models of seizures and epilepsy used in the discovery and development of new antiepileptic drugs. *Seizure-Eur. J. Epilep.* **2011**, *20*, 359−368.
(55) Potschka, H. Animal models of drug-resistant epilepsy. *Epileptic Disord.* **2012**, *14*, 226−234.
(56) Barton, M. E.; Klein, B. D.; Wolf, H. H.; Steve White, H. Pharmacological characterization of the 6 Hz psychomotor seizure model of partial epilepsy. *Epilepsy Res.* **2001**, *47*, 217−227.
(57) Bankstahl, M.; Bankstahl, J. P.; Löscher, W. Pilocarpine-induced epilepsy in mice alters seizure thresholds and the efficacy of antiepileptic drugs in the 6-Hertz psychomotor seizure model. *Epilepsy Res.* **2013**, *107*, 205−216.
(58) Li, P.; Chen, Z.; Xu, H.; Sun, H.; Li, H.; Liu, H.; Yang, H.; Gao, Z.; Jiang, H.; Li, M. The gating charge pathway of an epilepsy-associated potassium channel accommodates chemical ligands. *Cell Res.* **2013**, *23*, 1106−1118.
(59) Adler, M. W. Laboratory Evaluation of Antiepileptic Drugs. *Epilepsia* **1969**, *10*, 263−280.
(60) Leclercq, K.; Kaminski, R. M. Genetic background of mice strongly influences treatment resistance in the 6 Hz seizure model. *Epilepsia* **2015**, *56*, 310−318.
(61) Löscher, W.; Schmidt, D. Modern antiepileptic drug development has failed to deliver: Ways out of the current dilemma. *Epilepsia* **2011**, *52*, 657−678.

https://doi.org/10.1021/acs.jmedchem.0c02252
J. Med. Chem. 2021, 64, 5816−5837